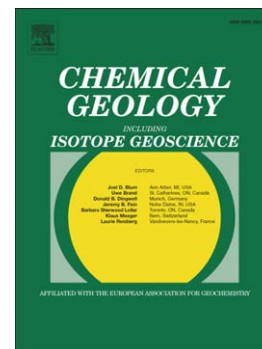# Accepted Manuscript

Influence of glaciation on mechanisms of mineral weathering in two high Arctic catchments

Ruth S. Hindshaw, Tim H.E. Heaton, Eric S. Boyd, Melody L. Lindsay, Edward T. Tipper

Please cite this article as: Hindshaw, Ruth S., Heaton, Tim H.E., Boyd, Eric S., Lindsay, Melody L., Tipper, Edward T., Influence of glaciation on mechanisms of mineral weathering in two high Arctic catchments, *Chemical Geology* (2015), doi: 10.1016/j.chemgeo.2015.11.004

This is a PDF file of an unedited manuscript that has been accepted for publication. As a service to our customers we are providing this early version of the manuscript. The manuscript will undergo copyediting, typesetting, and review of the resulting proof before it is published in its final form. Please note that during the production process errors may be discovered which could affect the content, and all legal disclaimers that apply to the journal pertain.

Influence of glaciation on mechanisms of mineral weathering in two high Arctic catchments

Ruth S. Hindshaw[a,*], Tim H. E. Heaton[b], Eric S. Boyd[c], Melody L. Lindsay[c], Edward T. Tipper[d]

[a]*Department of Earth and Environmental Sciences, University of St. Andrews, St. Andrews, UK*
[b]*NERC Isotope Geosciences Laboratory, Nottingham, UK*
[c]*Department of Microbiology and Immunology, Montana State University, Bozeman, Montana, USA*
[d]*Department of Earth Sciences, University of Cambridge, Cambridge, UK*

Abstract

In order to investigate the effect of glaciation on mineral weathering, the stream water chemistry and the bacterial community composition were analysed in two catchments containing nominally identical sedimentary formations but which differed in the extent of glaciation. The stream waters were analysed for major ions, δ^{34}S, δ^{18}O$_{SO4}$ and δ^{18}O$_{H2O}$ and associated stream sediments were analysed by 16S rRNA gene tagged sequencing.

Sulfate comprised 72-86% and 35-45% of the summer anion budget (in meq) in the unglaciated and glaciated catchments respectively. This indicates that sulfuric acid generated from pyrite weathering is a significant weathering agent in both catchments. Based on the relative proportions of cations, sulfate and bicarbonate, the stream water chemistry of the unglaciated catchment was found to be consistent with a sulfide oxidation coupled to silicate dissolution weathering process whereas in the glaciated catchment both carbonates and silicates weathered via both sulfuric and carbonic acids.

Stable isotope measurements of sulfate, together with inferences of metabolic processes catalysed by resident microbial communities, revealed that the pyrite oxidation reaction differed between the two catchments. No δ^{34}S fractionation relative to pyrite was observed in the unglaciated catchment and this was interpreted to reflect pyrite oxidation under oxic conditions. In contrast, δ^{34}S and δ^{18}O$_{SO4}$ values were positively correlated in the glaciated catchment and were positively offset from pyrite. This was interpreted to reflect pyrite oxidation under anoxic conditions with loss of S intermediates.

This study suggests that glaciation may alter stream water chemistry and the mechanism of pyrite oxidation through an interplay of biological, physical and chemical factors.

Keywords:

chemical weathering, pyrite, sulfur isotopes, bacteria, biogeochemical cycles

*corresponding author
Email address:* rh71@st-andrews.ac.uk (Ruth S. Hindshaw)

1. Introduction

The Arctic is currently experiencing a period of warming, resulting in the retreat of glaciers and an increase in the active layer depth of permafrost (Vaughan et al., 2013). Major emphasis has been placed on quantifying the effects of warming on nutrient fluxes, especially carbon (e.g. Schuur et al., 2009; Elberling et al., 2013), but major ion fluxes from both permafrost and glaciated areas (MacLean et al., 1999; Frey and McClelland, 2009; Pokrovsky et al., 2012; Nowak and Hodson, 2015) are also predicted to change with continued warming. Decreased permafrost cover is expected to increase overall fluxes of solutes as the active layer deepens (MacLean et al., 1999; Frey and McClelland, 2009). Likewise, solute fluxes from glaciers are predicted to increase by virtue of the increased discharge as a result of a longer melt season (Lafrenière and Sharp, 2005). However, it is unclear if, in addition to an increase in solute flux, the composition of this flux will change and what affect these changes will have on the carbon cycle and the microbial community which mediate many of the chemical reactions occurring in these environments (Skidmore et al., 2005; Boyd et al., 2011, 2014).

Chemical weathering, which is a key part of the biogeochemical cycles of many elements, is assumed to mainly occur by reaction with carbonic acid, formed by the dissolution of carbon dioxide (CO_2) in water. However, where sulfide minerals e.g. pyrite (FeS_2) exist, sulfuric acid may form through the oxidation of sulfide, which can also result in mineral dissolution (Holland, 1978). Understanding which agent is responsible for mineral dissolution is important for understanding inputs to the sulfur biogeochemical cycle and for quantifying the contribution of sulfuric acid weathering to global chemical weathering fluxes (Berner and Berner, 1996). Chemical weathering by sufuric acid does not involve drawdown of atmospheric CO_2 and can even be a net source of CO_2 if carbonates are weathered. Therefore, if this reaction were significant on a global scale then the weathering-climate negative feedback would be weakened (Calmels et al., 2007; Li et al., 2008; Torres et al., 2014).

Sulfide oxidation coupled to carbonate dissolution (SOCD) is a key process determining stream water chemistry in the high physical erosion environment of glaciated catchments (Fairchild et al., 1999; Tranter et al., 2002; Sharp et al., 2002; Skidmore et al., 2005; Robinson et al., 2009; Wadham et al., 2010; Boyd et al., 2014). The high rates of physical erosion expose both the carbonate and pyrite grains allowing them to weather rapidly. In non-glaciated Arctic catchments, weathering is also strongly influenced by physical erosion processes such as frost shattering (Huh and Edmond, 1999; Hall et al., 2002) and where sulfide is present, sulfide oxidation is a key chemical weathering reaction (Elberling and Langdahl, 1998; Thorn et al., 2001; Calmels et al., 2007). Significant weathering by sulfuric acid is also observed in other high erosion settings such as Taiwan and the Himalayas (Wolff-Boenisch et al., 2009; Turchyn et al., 2013; Torres et al., 2014).

The stable isotopes of sulfate ($\delta^{34}S$ and $\delta^{18}O_{SO4}$) provide a useful tool with which to investigate the sources of sulfate and the reactions leading to sulfate formation (e.g. Mandernack et al., 2003; Calmels et al., 2007; Wadham et al., 2007; Turchyn et al., 2013). Based on stable isotope evidence, sulfate reduction was identified at Borup Glacier in Ellesmere Island, Canada due to supra-glacial sulfur springs (Grasby et al., 2003) and in a sub-glacial upwelling from

Finsterwalderbreen, Svalbard (Wadham et al., 2004) but not in the pro-glacial area of the same glacier (Wadham et al., 2007). However, bacterial sequencing data from other catchments has failed to detect sulfate reducing bacteria where water chemistry evidence suggested sulfate reduction was occurring (Skidmore et al., 2000, 2005). It is therefore not clear how widespread this reaction is in glaciated environments.

The chemical reactions involving sulfide oxidation and sulfate reduction are microbially mediated and it is only in the last 15 years that the diversity and functional importance of microorganisms in glacial landscapes has been recognised (e.g. Skidmore et al., 2000; Hodson et al., 2008). More recently, it has been shown that the microbial community composition is strongly influenced by bedrock composition and that the microbial community strongly influences solute chemistry (Larouche et al., 2012; Montross et al., 2013; Mitchell et al., 2013). In particular, the presence of FeS_2 was shown to be a dominant control on the composition of communities inhabiting the subglacial environment of Robertson Glacier, Canada (Mitchell et al., 2013), which likely reflects the utilisation of energy derived from mineral redox reactions to support primary productivity (Boyd et al., 2014). It is therefore probable that minerals which can serve as electron donors and acceptors play a key role in determining the composition of microbial communities, and by extension the chemical composition of solute fluxes, in other oligotrophic and obligately chemotrophic subglacial environments.

This study focusses on two adjacent catchments with nominally identical lithology: sedimentary rocks known to contain pyrite. One catchment was glaciated and the other was unglaciated and underlain by permafrost. We assume that the extent of glacial cover is the primary cause of differences in hydrology, biology and chemistry between the two catchments. The paired catchment approach provides clues to long-term changes in weathering processes induced by deglaciation. The aim of the study was to utilise the combination of stream water chemistry, S and O isotopes of sulfate, and molecular analyses of microbial community composition to investigate the formation of and the role of sulfuric acid weathering in the two catchments.

2. Description of field area

Svalbard is located in the Arctic Ocean. The archipelago has an arctic climate with a mean annual air temperature of -5 °C and mean annual precipitation of 180 mm (measured at Longyearbyen airport, Humlum et al., 2003). Permafrost is continuous throughout the islands and can be up to 500 m thick (Humlum et al., 2003). The two studied catchments are situated next to each other (Fig. 1) in the Paleogene sedimentary Central Basin of Svalbard. The sedimentary formations exposed in the catchments are from the Van Mijenfjorden group which is Paleocene to Eocene in age (66 - 33.9 Ma) and contain sandstones, siltstones and shale (Fig. 2, Major et al., 2000).

Dryadbreen has been retreating since the end of the Little Ice Age (~1890, Ziaja, 2001). The thermal regime of the glacier is expected to be cold-based with temperate patches, based on similar sized glaciers in the same area (Etzelmüller et al., 2000; Etzelmüller and Hagen, 2005). Between 1936 and 2006 the area of the glacier decreased from 2.59 to 0.91 km^2 leaving large terminal and lateral ice-cored moraines and a sandur in front of the glacier (Ziaja
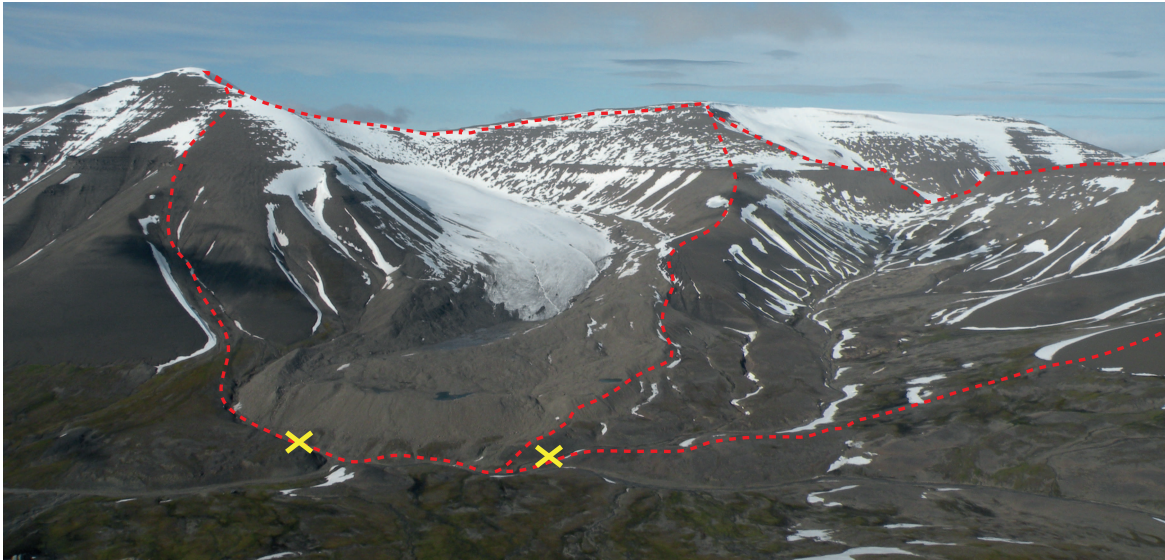
Figure 1: Panoramic view of the two study catchments. Dryadbreen is on the left and Fardalen on the right. The red dashed line demarcates the catchment boundaries and the yellow crosses indicate the water sampling locations for each catchment. Note the large end moraine and sandur in the glaciated catchment. Photograph credit: Alix Guillot.

and Pipała, 2007). The sandur surface lowered 14 m between 2001 and 2006 due to the melting of dead ice (Ziaja and Pipała, 2007). The uppermost part of the catchment faces north-north-east and the valley then curves around such that at lower elevations (<500 m) the catchment faces south-east. The catchment area is 4.8 km^2 and ranges in elevation from 250 - 1031 m.a.s.l. The river in the sandur plain is braided, but the braids merge such that one stream drains the end moraine. This stream was sampled just before the confluence with the river in the main valley. In this paper 'Dryadbreen' will be used to refer to the whole catchment and not just the glacier.

Fardalen is a non-glaciated catchment at the head of a valley of the same name. In contrast to Dryadbreen, the whole catchment has a south-easterly aspect which contributes to the absence of present-day glaciation. The valley is currently underlain by continuous permafrost and is likely to have been unglaciated for at least the last 10 kyr (Svendsen and Mangerud, 1997). The catchment area is 3.4 km^2 and ranges in elevation from 250 - 1025 m.a.s.l. A first-order stream drains the catchment and it was sampled just before the confluence with the river in the main valley.

3. Methods

3.1. Hydrology

Water stand and water temperature were recorded every 10 minutes by a CS450 Campbell Scientific pressure transducer connected to a Campbell CR200X data logger. In Dryadbreen conductivity was recorded every 10 minutes using a Ponsel CE4 meter. Water stand was converted to discharge using discharge measurements obtained by salt tracing, which were performed using a point addition of 1-3 kg salt. The resulting change in conductivity ∼70 m downstream was monitored by a Hobo U24 conductivity logger recording every second. The calibration of the
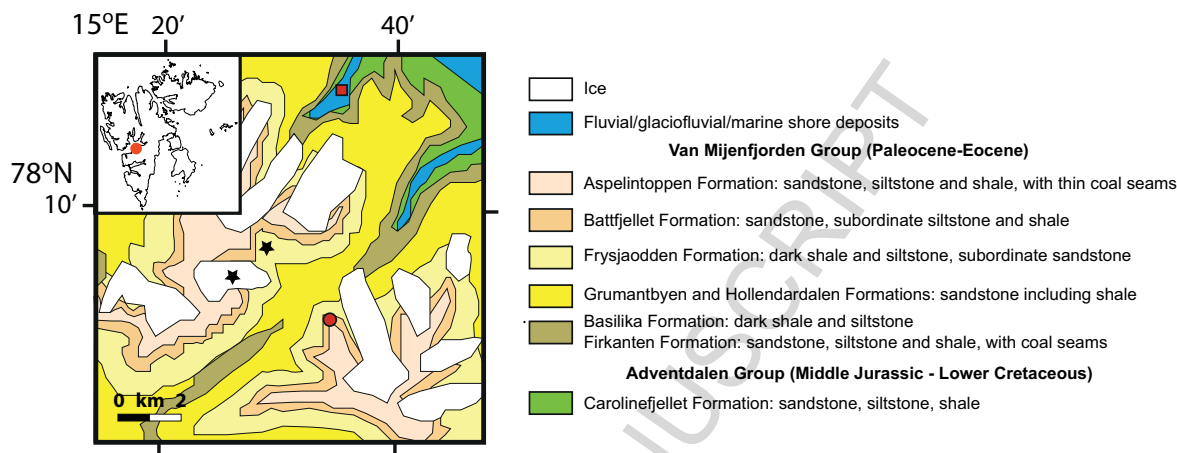
Figure 2: Geological map of the study area. The red dot in the inset shows the location of the study area in relation to the rest of Svalbard. The two stars indicate the location of the two catchments: Dryadbreen (glaciated) and Fardalen (unglaciated). The red square marks the location of Nybyen (part of the town of Longyearbyen) and the red circle shows from where the photograph in Figure 1 was taken. The map and the legend are from Major et al. (2000).

86 conductivity meter and conversion to discharge was done following the procedure outlined in Hudson and Fraser

87 (2005). The amount of snow in May 2012 prevented installation of the loggers that early in the season, therefore high

88 resolution hydrological data is only available for the period 25th July to 3rd August 2012. In mid-May there was no

89 surface water and no sub-surface water was found by digging. Three weeks later, the landscape was still dominated

90 by snow but both streams were flowing.

91 *3.2. Collection of water samples*

92   The Dryadbreen and Fardalen streams were sampled twice a day from 14th to 18th June 2012 and from 25th July

93 to 3rd August 2012. The number of days sampled corresponds to approximately 20% of the melt-season (Yde and

94 Knudsen, 2004). The two rivers were sampled just before they joined the main valley river. For Dryadbreen this

95 was approximately 1 km from the front of the glacier. Temperature and pH were measured in situ (Hanna HI 98160

96 pH meter). Water samples were filtered on the day of collection through 0.2 μm nylon filters using a polycarbonate

97 vacuum filtration unit connected to a hand pump. A filtered water sample was titrated with 3.3 mM HCl within an

98 hour of collection and alkalinity was calculated from the titration curve using the Gran method (Stumm and Morgan,

99 1996). Assuming that alkalinity $\approx$ [HCO_3^-]+[CO_3^{2-}] and using K_1, K_2, K_H values for 4 °C, then HCO_3^- comprises

100 more than 99.9% of alkalinity for all samples and we therefore assume that the measured alkalinity is equivalent to

101 the bicarbonate concentration. Filtered samples were stored in pre-cleaned HDPE bottles and those intended for the

102 analysis of cations were acidified to pH 2 with single-distilled concentrated HNO_3. Sulfate was pre-concentrated by

103 passing 3 L of filtered water through a column filled with 5 mL Dowex 1x8, 100-200 mesh chloride form resin. The

104 resin was pre-cleaned by rinsing with 60mL 3M HCl followed by 60 mL 18.2 MΩ water. Three snow samples were

105 taken by filling a bucket with snow and allowing it to melt at room temperature. Two rain samples were collected from

5

106 an HDPE bottle with a funnel. A supra-glacial stream sample was also collected. All of these samples were filtered
107 as described for river water samples.

3.3. Analysis of water samples

109 For all water samples, major cations and Si were measured by inductively-coupled plasma optical emission spec-
110 trometry (ICP-OES, Perkin Elmer Optima 5300 DV at the University of Edinburgh) and anions by ion chromatography
111 (IC, Dionex DX 500 at Durham University). Measured cation concentrations of the water standards SLRS-5 (National
112 Research Council Canada) and BATTLE-02 (Environment Canada) were within 8% of the certified values. Measured
113 anion concentrations were within 5% of the certified values for LETHBRIDG-03 and BATTLE-02 (both Environment
114 Canada). External reproducibility, as measured by the mean normalized difference of 9 pairs of replicate field samples,
115 was <3% for cations and <5% for anions. Calculated charge balance errors (CBE) were <3% for the vast majority of
116 samples, confirming the accuracy of the anion and cation measurements (Table 1).

117 The oxygen isotopic composition ($\delta^{18}O_{H2O}$) of water samples was measured on 750 μL samples of water which
118 had been equilibrated with a mixture of 0.3% CO_2 and He in septum capped vials. The CO_2/He mixture was measured
119 using a Gas Bench II (Thermo Scientific) connected to an isotope ratio mass spectrometer (IRMS, Delta PLUS XP,
120 Thermo Scientific at the University of St. Andrews). Measurements were calibrated with the international standards
121 SLAP-2, GISP and VSMOW-2. The results are reported in the conventional delta notation with respect to VSMOW
122 and sample standard deviation was less than 0.15‰ (2SD).

123 Sulfate from the anion resins was eluted with 2 M KCl, and the eluent acidified to pH 3 with HCl, heated to
124 sub-boiling, and barium sulfate precipitated by addition of $BaCl_2$. The barium sulfate was then recovered by four
125 cycles of centrifugation, discard of the supernatant, and washing in de-ionised water before oven drying at 80 °C. The
126 sulfate blank for the process is less than 0.5 mg $BaSO_4$ (limit of determination), which is less than 1% of the smallest
127 sample. $^{34}S/^{32}S$ ratios were determined by combustion to SO_2 with V_2O_5 in an EA-1120 elemental analyser on-line to
128 an IRMS (Delta+XL, ThermoFinnigan at the NERC Isotope Geosciences Laboratory), with $^{34}S/^{32}S$ ratios calculated
129 as $\delta^{34}S$ values versus CDT by comparison with standards IAEA SO6 and NBS-127. Analytical precision of replicates
130 was typically ≤0.2‰ (1 SD). $^{18}O/^{16}O$ ratios were determined by thermal conversion to CO in a TC/EA on-line to an
131 IRMS (Delta+XL, ThermoFinnigan at the NERC Isotope Geosciences Laboratory), with $^{18}O/^{16}O$ ratios calculated as
132 $\delta^{18}O_{SO4}$ values versus SMOW by comparison with standards IAEA SO5 and SO6. Analytical precision of replicates
133 was typically <0.5‰ (1 SD).

3.4. Analysis of solid samples

135 Three rock samples were collected: R01 was collected from the Frysjaodden Formation (Fig. 2) in Fardalen,
136 R02 was collected from the sandur in Dryadbreen and R04 was collected from the surface of the glacier. The rock
137 samples, in addition to a sediment sample taken at the water sampling location in each catchment (O - Dryadbreen
138 and L - Fardalen) were crushed and ground to fine powders. The rock samples were analysed by X-ray fluorescence

6

spectrometry (XRF, PANalytical Axios at the Norwegian Geological Survey) and all samples were analysed by X-ray diffraction (XRD). S contents of the rock samples were analysed by high temperature combustion followed by infrared detection (Leco SC-444 at the Norwegian Geological Survey). XRD analysis was performed on a PANalytical PW1050 X-ray diffractometer with a Hiltonbrooks DG2 X-ray generator (Co-Kα radiation) at the University of St. Andrews. Data were collected between 5 and 70° 2θ with a step size of 0.02° and a counting time of 3 s per step. Semi-quantitative mineralogical abundances were obtained using the Siroquant software. The typical error on abundances is estimated to be 5-10%. Carbon isotope analysis of calcite from R02 was performed by reaction of whole rock powder with anhydrous phosphoric acid overnight at 25 °C and subsequent analysis of the liberated CO_2 in a MAT 253 mass spectrometer (ThermoFinnigan at the NERC Isotope Geosciences Laboratory). $^{13}C/^{12}C$ ratios were converted to $\delta^{13}C$ values versus VPDB by comparison with a laboratory calcite standard calibrated against NBS-19 and NBS-18.

Pyrite was separated from two shale samples by using a solution of lithium heteropolytungstate (LST). The separated fraction contained both pyrite and magnetite and the pyrite was separated from magnetite using a magnet and hand-picking. Pyrite separates were ground to a powder in an agate mortar and $^{34}S/^{32}S$ ratios determined by combustion to SO_2 with V_2O_5 in an EA-1120 elemental analyser on-line to an IRMS (Delta+XL, ThermoFinnigan at the NERC Isotope Geosciences Laboratory), with $^{34}S/^{32}S$ ratios calculated as $\delta^{34}S$ values versus CDT by comparison with standards IAEA S-1 and S-2. Analytical precision of replicates was ≤0.4‰ (1 SD).

Suspended sediment samples (>0.2μm, collected on nylon filter papers) were washed off the filter papers using deionized water and freeze-dried. Depending on the amount of sediment recovered, part or all of the sample was then reacted overnight with 1.5 M HCl to remove carbonates, washed free of acid, dried and homogenised. $^{13}C/^{12}C$ ratios were determined by combustion to CO_2 in an EA-1120 elemental analyser on-line to an IRMS (Delta+XL, ThermoFinnigan at the NERC Isotope Geosciences Laboratory), with $^{13}C/^{12}C$ ratios calculated as $\delta^{13}C$ values versus VPDB by comparison with laboratory standards calibrated against NBS 19 and IAEA CH-7. Analytical reproducibility was typically ≤0.2‰ (1 SD).

Table 1: Summary of water chemistry and isotopic data. These data have not been corrected for precipitation inputs.

Sample (YYYYMMDD)	Time (local)	Discharge (m³ s⁻¹)	pH	T °C	Cond. (µS/cm)	CBE[1] %	Ca µmol/L	Mg	Na	K	Si	Cl⁻	F⁻	NO₃⁻	SO₄²⁻	HCO₃⁻	$\delta^{34}S$ ‰	$\delta^{18}O_{SO4}$	$\delta^{18}O_{H2O}$
Dryadbreen (glaciated) - spring																			
20120615D	11:26		6.91	0.1	56.9	-1	125	124	188	11	13	208	4	8	113	263	-0.57	-6.0	-15.28
20120616D	18:18		6.06	0.1	36.4	-1	92	92	137	10	11	137	4	3	85	212	+0.73	-5.4	-14.58
20120617D	10:20		5.94	0.3	61.2	0	96	93	160	14	12	190	4	6	75	195			-15.06
20120618D	09:40					-1	99	88	167	9	12	208	4	9	65	210			-15.46
Dryadbreen (glaciated) - summer																			
20120725D	10:10		6.76	2.9	35.3	-3	108	100	85	14	8	40	4	2	94	315	-2.02	-7.7	-13.96
20120726D	20:11	0.43	7.30	1.3	39.0	-3	120	111	97	8	8	40	4	2	111	331			-13.79
20120727D	09:00	0.28	7.18	2.7	50.0	-3	141	131	107	10	9	42	4	3	137	372	-2.28	-8.1	-13.83
20120728D	19:28	0.50	5.70	2.0	39.5	1	116	105	87	8	9	34	4	2	116	249			-13.49
20120729D	08:45	0.35	6.34	2.1	39.0	0	115	106	94	8	8	36	4	2	110	284	-2.31	-8.0	-13.54
20120730D	19:22	0.46	6.94	1.1	36.3	-2	117	108	87	8	8	37	4	2	111	307			-13.04
20120731D	08:37	0.25	6.91	2.6	52.6	0	144	135	111	11	13	44	4		141	349	-2.64	-9.7	-13.41
20120801D	16:17	0.39	6.86	3.6	33.5	7	109	98	80	9	8	37	4	1	90	212			-13.28
20120802D	08:50	0.36	6.89	1.6	46.1	5	137	125	131	17	11	53	4		124	299	-2.28	-8.5	-13.22
20120803D	19:10	0.38	6.70	2.0	49.4	0	142	130	95	12	9	37	4		132	346			-13.72
Fardalen (unglaciated) - spring																			
20120614F	10:26		7.37	0.1	129.1	-1	213	253	323	16	29	226	8	14	461	130	-3.56	-8.1	-15.76
20120615F	17:46		7.34	0.0	117.0	0	198	233	312	15	29	181	5	11	419	151			-15.43
20120616F	10:25		7.22	0.0	84.5	-1	147	176	255	11	21	174	4	10	313	116	-3.66	-8.1	-15.46
20120617F	16:28		5.70	0.1	66.0	-1	138	160	233	12	25	148	5	8	288	124			-15.17
20120618F	09:35		6.20	0.1	58.3	-2	136	156	230	11	27	133	5	7	287	134	-3.40	-8.4	-15.15
Fardalen (unglaciated) - summer																			
20120725F	18:51		7.12	2.8	82.5	0	172	191	167	12	28	30	5	4	323	225	-3.65		-13.65
20120726F	09:10	0.24	6.30	2.2	108.3	0	218	245	202	13	32	40	8	6	423	241		-9.7	-13.60
20120727F	19:32	0.27		3.3	119.7	2	236	267	211	14	33	43	8	6	459	219			-13.47
20120728F	09:05	0.14	5.82	3.5	135.9	4	257	292	238	15	34	43	9	6	529	135	-7.08	-9.5	-13.43
20120729F	19:19	0.38	6.27	3.2	99.6	1	200	224	182	12	29	31	5	4	374	239			-13.21
20120730F	09:30	0.26	6.70	2.3	112.9	1	216	248	206	13	30	38	8	4	438	201	-7.03	-9.7	-13.05
20120731F	18:10	0.38	6.82	5.0	126.2	1	252	283	205	15	37	47	8	5	475	259			-13.03
20120801F	08:35	0.23	7.15	5.3	162.2	1	298	344	282	18	37	47	9	7	640	223	-7.66	-10.1	-13.26
20120802F	19:35	0.14	6.85	3.2	150.3	-1	280	318	247	16	33	44	9		584	269		-10.1	-13.17
20120803F	08:55	0.14	6.87	3.3	156.1	-2	283	323	253	15	34	46	9	7	602	265	-7.12		-13.45
Supra-glacial sample																			
20120801SG	13:50						10	9	16	1	1	14	3		9				-13.98
Snow samples																			
20110713S							8	6	32	7	1	31			9				-12.87
20120527S							1	2	20	1	0	12		1	8				17.01
20120614S							1	0	14	2	0	14			8				-20.24
Rain samples																			
20120724R							16	5	19	9	1	19	3	4	13				-16.49
20120803R							32	6	53	13	0	75	3	4	15				-14.36

[1] CBE = charge balance error = $((\Sigma^+ - \Sigma^-)/(\Sigma^+ - \Sigma^-)) \times 100$ in meq

8

3.5. Sequencing of bacterial 16S rRNA genes

Four surface sediment samples were sequenced: two from Fardalen collected in spring at the water sampling location, L (river sediment) and M (sediment by the side of the river resting on snow) and two from Dryadbreen collected in summer, A (sediment from a pool of water in the sandur, not connected to main river) and O (sediment adjacent to the river at water sampling location). Sediment samples were scooped directly into either sterile 300 mL PVC containers or sterile 50 mL centrifuge tubes. The samples were stored at ambient temperature (<4 °C) until they were transported to the lab where they were desiccated by drying at 40 °C (4 days). Desiccated samples were shipped internationally to the USA where they were subjected to molecular analyses.

Nucleic Acid Extraction and Quantification. DNA extraction and purification were carried out with a Fast DNA Spin Kit for Soil (MP Biomedicals, Solon, OH). DNA was extracted in triplicate from three independent 250 mg subsamples of sediment. Equal volumes of each replicate extract were pooled and the concentration of DNA was determined using a Qubit dsDNA HS Assay kit (Molecular Probes, Eugene, OR) and a Qubit 2.0 Fluorometer (Invitrogen, Carlsbad, CA).

PCR Amplification of bacterial and archaeal 16S rRNA Genes from Genomic DNA. Purified genomic DNA extracts were subjected to amplification of bacterial and archaeal 16S rDNA using primers 344F (5'-ACGGGGYGCAGCAGGCGCGA-3') and 915R (5'-GTGCTCCCCCGCCAATTCCT-3') at an annealing temperature of 61°C or 1100F (5'-YAACGAGCGCAACCC-3') and 1492R (5'-GGTTACCTTGTTACGACTT-3') at an annealing temperature of 55 °C, respectively (Boyd et al., 2007). Approximately 1 ng of purified genomic DNA was subjected to PCR in triplicate using the following reaction conditions: initial denaturation at 94 °C (4 min), followed by 35 cycles denaturation at 94 °C (1 min), annealing at the optimal temperature for the primer pair (1 min), primer extension at 72 °C (1.5 min), followed by a final extension step at 72 °C for 20 min. Reactions contained 2 mM MgCl$_2$ (Invitrogen, Carlsbad, CA), 200 μM each deoxynucleotide triphosphate (Eppendorf, Hamburg, Germany), 0.5 μM forward and reverse primer (Integrated DNA Technologies, Coralville, IA), 0.4 mg ml^{-1} molecular-grade bovine serum albumin (Roche, Indianapolis, IN), and 0.25 units Taq DNA polymerase (Invitrogen, Carlsbad, CA) in a final reaction volume of 50 μL. Positive control reactions were performed using genomic DNA from *Azotobacter vinelandii* DJ and *Sulfolobus solfataricus* P2. Negative control reactions were performed in the absence of added genomic DNA. PCR amplicons were only obtained from extracts when bacterial primer sets were applied. Archaeal 16S rRNA gene amplicons were not recovered from any of the four sediment DNA extracts.

Sequencing and analysis of bacterial 16S rRNA genes. Bacterial 16S rDNA amplicons were sequenced by Molecular Research LC (Lubbock, TX). 16S rDNA from each site were barcoded and were sequenced using a 454 Genome Sequencer FLX System. Post sequence processing was performed using the Mothur (ver. 1.33.3) sequence analysis platform (Schloss et al., 2009). Raw libraries were trimmed to a minimum length of 250 bases and were subjected to a filtering step using the quality scores file to remove sequences with anomalous base calls. Unique sequences were aligned using SILVA databases and sequences were trimmed using a defined start and end sites and a maximum length of 250 bases. The resulting unique sequences were pre-clustered to remove amplification and sequencing errors

9

and chimeras were identified and removed using UCHIME (Edgar et al., 2011). Operational taxonomic units (OTUs) were assigned at a sequence similarity of 0.03 using the furthest-neighbour method. The remaining sequences were randomly sub-sampled in order to normalize the total number of sequences in each library. Collectively, these steps resulted in a normalized size of 1077 bacterial 16S rRNA gene sequences for each assemblage. Sequences were classified using the Bayesian classifier (Wang et al., 2007) and the RDP database, with manual verification using BLASTn (Supp. Table 1). Sequences representing each OTU have been deposited in the NCBI SRA database under accession number SRR1562043.

Sequences representing each unique OTU (defined at 0.03% sequence identities) were compiled for each domain. ClustalX (ver. 2.0.9, Larkin et al., 2007) was used to align nucleic acid sequences using default parameters and the alignment was subjected to evolutionary model prediction via jModeltest (ver. 2.1.1, Darriba et al., 2012), Maximum-Likelihood phylogenetic reconstruction via PhyML (version 3.0, Guindon and Gascuel, 2003) specifying the general time reversible model and gamma distributed rate variation with a proportion of invariable sites, and rate smoothing using the multidimensional version of Rambaut's parameterization as implemented in PAUP (ver. 4.0, Swofford, 2001) as previously described (Meuser et al., 2013). Phylocom was used to calculate Rao's community phylogenetic relatedness for the bacterial assemblages using relative sequence abundance weights and the rate-smoothed ultrameric tree. PAST (ver. 1.72, Hammer et al., 2001) was used to generate cluster dendograms specifying single linkage and Euclidean distances. Bootstrap values correspond to the frequency that each node was observed in a given position out of 1000 replicates.

3.6. Precipitation correction

Snow is the primary source of precipitation to the two studied catchments, but the chemical composition of the water derived from melting snow varies temporally (e.g. Johannessen and Henriksen, 1978). Therefore instead of using the snow samples collected for this study, which were collected relatively late in the season as a measure of precipitation inputs, we compiled literature data on pre-melt Svalbard snow-pack chemistry (Hodgkins et al., 1997; Wynn et al., 2006; Tye and Heaton, 2007; Yde et al., 2008). Pre-melt snow-pack samples are typically taken in April and are assumed to represent "fresh" snow. From these data average X/Cl ratios were calculated, without any weighting, where X is a major cation or anion. By assuming that chloride is conservative and only derived from precipitation, the stream water data are corrected for snow inputs using the following formula:

$$X^* = X_{river} - (X/Cl)_{snow} \cdot Cl_{river} \tag{1}$$

where X^* and X_{river} denote precipitation-corrected and uncorrected concentrations respectively. The X/Cl ratios used for the precipitation correction were ($\pm$1SD, n=8-10): Ca/Cl 0.11$\pm$0.10, Mg/Cl 0.09$\pm$0.04, Na/Cl 0.85$\pm$0.09, K/Cl 0.02$\pm$0.01 and SO$_4$/Cl 0.11$\pm$0.04. The propagated error on the precipitation corrected values in summer was less than 7% (RSD) for K and Na and less than 4% (RSD) for Ca, Mg and SO$_4$. In spring, the propagated error was higher

10

Table 2: Precipitation-corrected $\delta^{34}S$ and $\delta^{18}O_{SO4}$ values ($\delta^{34}S^*$ and $\delta^{18}O_{SO4}^*$).

Sample (YYYYMMDD)	SO_4 in precipitation %	$\delta^{34}S$ ‰	$\delta^{34}S^*$ ‰	$\delta^{18}O_{SO4}$ ‰	$\delta^{18}O_{SO4}^*$ ‰
Dryadbreen (glaciated) - spring					
20120615D	21.3	-0.6	-4.5	-6.0	-10.2
20120617D	29.0	0.7	-4.7	-5.4	-11.5
Dryadbreen (glaciated) - summer					
20120725D	4.8	-2.0	-2.8	-7.7	-8.6
20120727D	3.5	-2.3	-2.9	-8.1	-8.7
20120729D	3.8	-2.3	-2.9	-8.0	-8.7
20120731D	3.6	-2.6	-3.2	-9.7	-10.4
20120802D	4.9	-2.3	-3.1	-8.5	-9.4
Fardalen (unglaciated) - spring					
20120614F	5.6	-3.6	-4.6	-8.1	-9.2
20120616F	6.4	-3.7	-4.9	-8.1	-9.2
20120618F	5.3	-3.4	-4.4	-8.4	-9.4
Fardalen (unglaciated) - summer					
20120726F	1.1	-6.7	-6.9	-9.7	-9.9
20120728F	0.9	-7.1	-7.3	-9.5	-9.7
20120730F	1.0	-7.0	-7.2	-9.7	-9.9
20120801F	0.8	-7.7	-7.8	-10.1	-10.2
20120803F	0.9	-7.1	-7.3	-10.1	-10.2

due to the greater amount of snow-melt and the error was consistently higher in Dryadbreen. Errors were less than 25% (RSD) except for Na in Dryadbreen which were closer to 50% (RSD). The $\delta^{34}S$ and $\delta^{18}O_{SO4}$ values were also corrected for snow inputs (Table 2). Reported values for the $\delta^{34}S$ composition of snow in Svalbard vary from +11.5 to +18.0‰ (Tye and Heaton, 2007). To estimate a value of $\delta^{34}S$ for the snow pack we took the percentage of SO_4 derived from snow for the spring samples and extrapolated to a $\delta^{34}S$ value at 100% SO_4 from snow (Fig. 3). The value estimated for snow using this approach was +14‰ which is within the range previously reported (Tye and Heaton, 2007). Using this value, $\delta^{34}S$ values were corrected using the following formula:

$$\delta^{34}S^* = (\delta^{34}S_{river} - f \cdot \delta^{34}S_{snow})/(1 - f) \tag{2}$$

where f is the fraction of SO_4 from snowmelt. $\delta^{18}O_{SO4}$ values were corrected in an identical manner to that described above for $\delta^{34}S$ using a snow value of +9.5‰ based on a fresh snow sample from Svalbard (Tye and Heaton, 2007). Unless otherwise stated, precipitation-corrected values are used in all figures in this manuscript and are indicated by an asterisk.

4. Results

4.1. Water chemistry and hydrology

The water samples taken in spring were dominated by snow-melt as evinced by the high proportion of Cl and Na compared to the summer samples (Fig. 4, Table 1). The most abundant anion in Dryadbreen was HCO_3^- which comprised 48-58% of the major anions (in meq) in summer. This was in stark contrast to Fardalen where SO_4^{2-} was the major anion comprising 72-86% of the major anions (in meq) in summer (Fig. 4). The precipitation corrected
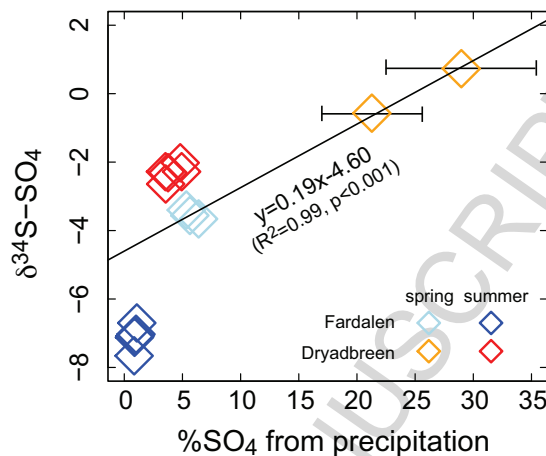
11

Figure 3: Stream water δ^{34}S values against the calculated %SO$_4$ derived from precipitation. The regression line is derived from the spring samples only. The δ^{34}S value when 100% SO$_4$ is derived from precipitation is +14‰ which is comparable with the +11.5 to +18.0‰ range reported for snow (fresh snow and snow-pack) from Svalbard by Tye and Heaton (2007). The δ^{34}S value when 0% SO$_4$ is derived from precipitation is -4.6±0.2‰ and is assumed to represent sulfate derived from a pyrite weathering source. The summer samples do not lie on the mixing line between snow and a pyrite source which either indicates additional pyrite sources with different δ^{34}S values or fractionation processes. Error bars smaller than symbol size are not depicted.

²⁴⁵ abundances of cations were similar in both catchments (Fig. 4). In Dryadbreen precipitation sources accounted for

²⁴⁶ 34-48% of the cation abundance (in meq) in spring and 10% in summer. In Fardalen, the precipitation contribution

²⁴⁷ to the cation abundance was slightly less: 19-29% in spring and 4% in summer. The abundances of Ca and Mg were

²⁴⁸ very similar in both catchments but in Fardalen Mg was consistently more abundant compared to Dryadbreen where

²⁴⁹ Ca was most abundant. The total dissolved load of Fardalen (53±7 mgL^{-1}, 1SD) was approximately double that of

²⁵⁰ Dryadbreen (25±4 mgL^{-1}, 1SD).

²⁵¹ The δ^{18}O$_{H2O}$ value of the stream water varied from around -15‰ in spring to around -13‰ in summer (Table 1),

²⁵² reflecting the decrease in snow cover from spring to summer (Hindshaw et al., 2011). There is no significant differ-

²⁵³ ence in δ^{18}O$_{H2O}$ values between the two catchments reflecting a common precipitation source. The sulfur isotopic

²⁵⁴ composition of sulfate (δ^{34}S) decreased from spring to summer: from +0.73 to -2.64‰ in Dryadbreen and from -3.40

²⁵⁵ to -7.66‰ in Fardalen (Table 1). Similar to δ^{34}S values, δ^{18}O$_{SO4}$ values exhibited a seasonal shift towards lower

²⁵⁶ values in summer with the lowest value (-10.1‰, Table 1) measured in Fardalen.

²⁵⁷ The discharge of both streams at the time of sampling is given in Table 1. Both streams exhibit diurnal cycles in

²⁵⁸ discharge and the range of discharge measured in both catchments was 0-0.5 m^{3}s^{-1} (not including periods of logger

²⁵⁹ malfunction), but the median discharge over the period of data collection for Dryadbreen (0.40 m^{3}s^{-1}) was greater

²⁶⁰ than for Fardalen (0.22 m^{3}s^{-1}).

12

Table 3: XRF data for rock samples.

Sample	Class[1]	Fm.[2]	SiO_2 wt%	Al_2O_3 wt%	Fe_2O_3 wt%	TiO_2 wt%	MgO wt%	CaO wt%	Na_2O wt%	K_2O wt%	MnO wt%	P_2O_5 wt%	LOI[3] wt%	Total wt%
R01	Shale	Fry.	63.2	16.3	7.1	0.8	1.4	0.3	1.0	2.6	0.1	0.3	7.5	101.0
R02	Wacke	Batt.	65.4	13.0	7.9	0.6	1.5	0.6	0.7	2.2	0.1	0.3	7.2	99.5
R04	Shale	Fry.	57.1	19.1	3.5	0.9	1.3	0.2	0.6	3.6	0.0	0.1	12.9	99.3

[1] Classification using SandClass for terrigenous sands and shales (Herron, 1988).
[2] Formation assignment based on Schlegel et al. (2013). Fry. = Frysjaodden Formation and Batt. = Battfjellet Formation.
[3] LOI = Loss on Ignition.

4.2. Solid samples

Based on the SandClass system for terrigenous sand and shale samples (Herron, 1988), R01 and R04 were classified as shales and R02 as a wacke (Table 3). Schlegel et al. (2013) have previously classified rock core samples from the Frysajodden Formation as shales and those from the Battfjellet and Aspelintoppen formations as wackes and litharenites respectively. We therefore assume that R01 and R04 originated from the Frysajodden Formation and R02 from the Battfjellet Formation (Fig. 2). The main minerals in the bulk rock and sediment samples analysed by XRD were quartz, plagioclase, chlorite, kaolinite, illite/mica and illite/smectite (Table 4). Clay minerals accounted for 44% (sediment O) to 65% (R04) of the total composition. Calcite abundance was below 1% in all samples analysed. However, calcite was detected in XRD analysis of orientated clay fractions from river sediments collected in the glaciated catchment (Dryadbreen) but not in sediments collected from the unglaciated catchment (Fardalen). The low calcite abundance is in agreement with previous studies which report <1-2% carbonate in core samples from these formations (Dypvik et al., 2011; Schlegel et al., 2013). Calcite in rock sample R02 had a δ^{13}C value of -1.7‰ (Table 5). The δ^{13}C values of suspended sediments show neither temporal nor spatial variation and the average value of -26‰ (Table 5) reflects carbon fixed by the Calvin-Benson-Bassham cycle (C3) which may be of plant (Kendall and Doctor, 2003) or microbial origin (Havig et al., 2011).

Pyrite was detected in the bulk phase XRD analysis of R02 (Table 4) and was separated from both R01 and R02. No gypsum was detected by XRD analysis and none was detected in thin sections from these same formations (Dypvik et al., 2011; Schlegel et al., 2013). The S content of R01 and R02 was 0.02 and 0.90 wt% respectively. Assuming that all the S is from pyrite with a formula FeS_2, then this corresponds to 0.04 and 1.69 wt% pyrite in the two rocks samples, in agreement with the XRD data (Table 4). It is therefore highly likely that pyrite is the main S-bearing mineral phase in these rock samples. The δ^{34}S values of pyrite mineral separates from samples R01 and R02 were -5.4±0.4‰ and -7.6±0.2‰ (1SD) respectively (Table 5). The difference in values is likely due to the two samples being derived from different formations (Table 3).

4.3. Bacterial community composition

The phylogenetic affiliation of the 16S rRNA genes recovered from the sediment samples, as determined by BLASTn analysis, are depicted in Fig. 5.

13

Table 4: Semi-quantitative mineral abundances (% total) in rock and sediment samples.

| Mineral | Sample | | | | |
	R01	R02	R04	O[1]	L[1]
Quartz	38	46	31	51	40
Plagioclase	7	3	3	5	6
K-Feldspar	<1	<1	1	<1	<1
Chlorite	9	8	11	12	5
Illite/Mica	26	24	28	17	32
Illite/Smectite	8	7	9	<3	<3
Kaolinite	12	9	17	15	17
Pyrite	<1	1	<1	<1	<1
Siderite	<1	3	<1	<1	<1
Calcite	<1	<1	<1	<1	<1

[1]O = Dryadbreen sediment, L = Fardalen sediment

Table 5: Summary of C contents and C and S isotope data of solid samples.

Sample	C wt%	1SD*	δ^{13}C ‰	1SD*	δ^{34}S ‰	1SD*
>0.2μm suspended sediments						
Dryadbreen (glaciated)						
20120615D#	4.07		-26.1			
20120617D#	2.88		-26.3			
20120725D	2.17		-25.6			
20120725D#	2.33	0.10	-26.2	0.1		
20120727D#	2.17		-26.2			
20120729D	2.60		-25.7			
20120729D#	2.64	0.25	-26.2	0.0		
20120731D	2.46		-25.6			
20120731D#	2.30	0.10	-26.2	0.1		
20120802D#	2.54		-26.4			
Fardalen (unglaciated)						
20120616F#	2.43		-26.4			
20120618F#	2.02		-26.6			
20120726F#	2.59		-26.8			
20120728F#	2.63		-26.0			
20120730F#	2.49		-26.5			
Pyrite mineral separates						
R01					-5.4	0.4
R02					-7.6	0.2
Calcite mineral separate						
R02			-1.7			

*Errors reported where there was enough sample material
for repeat measurements.
# Denotes that sample was treated with 5% HCl to remove
carbonates.

Clear differences were observed in the composition of sediment associated bacterial communities that were submerged in the stream versus those that were collected on the banks of the stream. For example, samples M (Fardalen, sediment on snow adjacent to river) and O (Dryadbreen, sediment adjacent to river) both comprised large numbers of firmicutes, whereas the two samples collected under water (A and L) contained very low abundances of these lineages (Fig. 5b). A (Dryadbreen) and L (Fardalen) were dominated by sequences affiliated with Proteobacteria (48 and 65% of the total bacterial community, respectively) with those affiliated with Betaproteobacteria representing the most abundant proteobacterial class (21% and 31% respectively). Sequencing studies from glaciated environments have found that Betaproteobacteria are the dominant phylogenetic group in subglacial and proglacial sediments where they are likely to be involved in S and Fe cycling under oxic conditions (Foght et al., 2004; Skidmore et al., 2005;
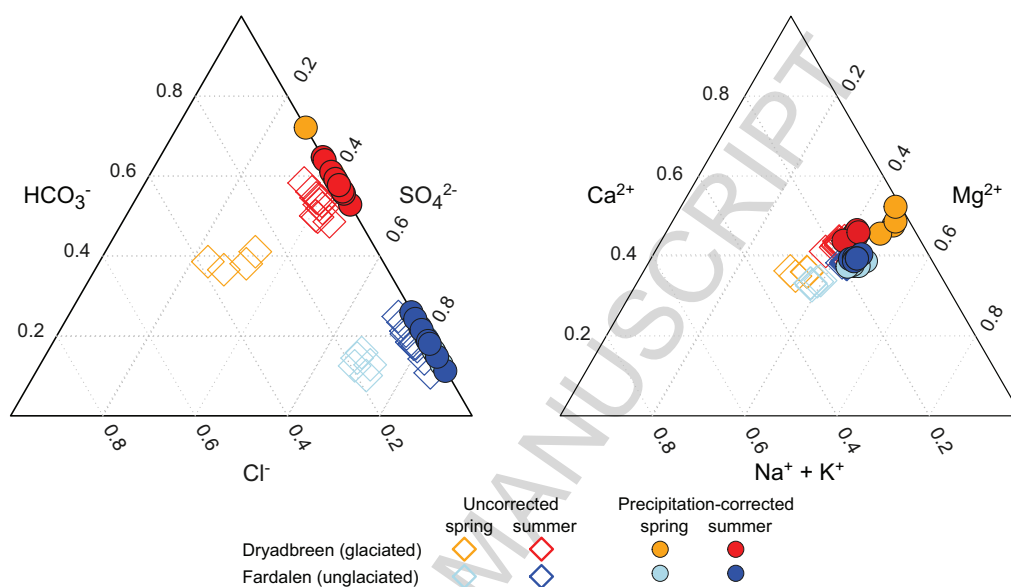
Figure 4: Major ion water chemistry (in meq) shown in ternary diagrams. Uncorrected data are shown as open diamonds and precipitation corrected data are shown as filled-in circles. The data are further divided into samples collected in spring and those collected in summer. The striking difference between the two catchments is in their relative anion abundances with Dryadbreen (glaciated) dominated by HCO_3^- and Fardalen (unglaciated) dominated by SO_4^{2-}. Error bars are smaller than the symbols.

Mitchell et al., 2013).

Differences in the composition of the bacterial communities associated with sediments sampled from the two submerged sites A (Dryadbreen) and L (Fardalen) were also apparent. For example, sequences affiliated with the anaerobic phylum Bacteriodetes represented the most abundant phylum (24%) in the community sampled from Dryadbreen (A), whereas Bacteriodetes represented only a minor fraction of the community (3%) from Fardalen (L). This may indicate a shift toward more anaerobic metabolisms in the proglacial sediment bacterial communities at Dryadbreen.

In the discussion we will focus on sediment samples A and L as representative of each catchment since they were collected under water and therefore are most likely to be adapted to or responsible for the differences in water chemistry observed between the two catchments.

5. Discussion

5.1. Overall weathering reactions

The most obvious difference between the two streams is in the anion composition: Dryadbreen is dominated by HCO_3^-, whereas Fardalen is dominated by SO_4^{2-}. This indicates that different weathering reactions are occurring in the two catchments despite nominally identical lithology. A first indication of which weathering reactions are important for each catchment can be gained by looking at element ratios since the reactions of carbonates and silicates
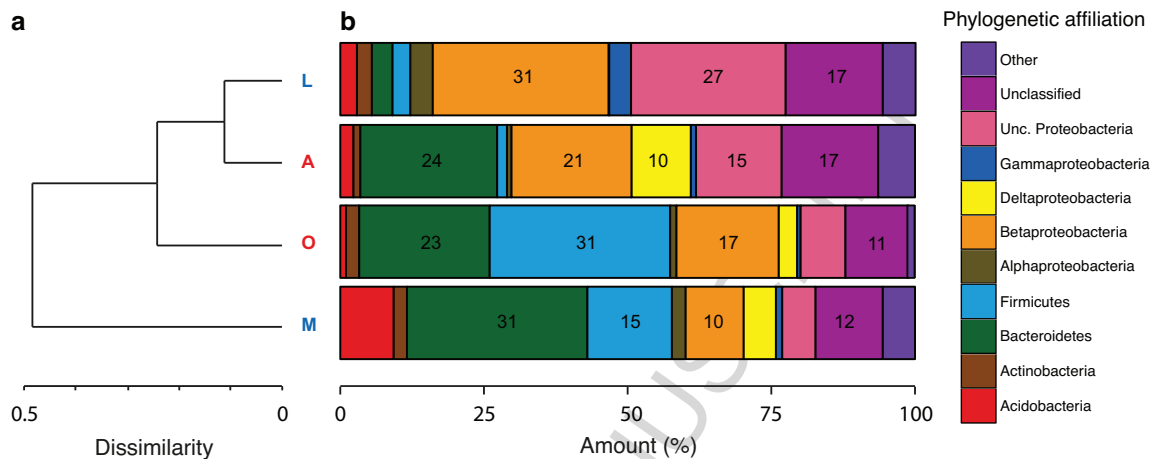
15

Figure 5: (a) Dendrogram based on the Rao phylogenetic diversity index (Rao, 1982) which depicts the degree of phylogenetic dissimilarity between the bacterial communities associated with the different sediment samples. Samples A and O were collected in Dryadbreen (red letters) and L and M were collected in Fardalen (blue letters). Samples A and L were collected under water and form a cluster, indicating they are more similar in their bacterial phylogenetic composition as compared to samples O and M. Sample O was collected adjacent to the river and sample M was collected adjacent to the river but on top of snow. (b) Relative abundance of bacterial phyla or classes (Proteobacteria only) based on percent identities to their closest cultivated sequence, as determined by BLASTn analysis. The phyla Armatimonadetes, Chlamydiae, Gemmatimonadetes, Nitrospinae, Nitrospira, Nitrospirales, Planctomycetes, TM7, Verrucomicrobia and WS3 are grouped together in 'Other'.

with either carbonic or sulfuric acids will give distinct ratios of cations versus SO_4^{2-} and HCO_3^- (Fairchild et al., 1994; Tranter et al., 2002; Wadham et al., 2010). Example reactions and their corresponding slopes in units of equivalents (eq) are presented below (Eqns. 3-6) and in Table 6. Feldspars are the primary silicate minerals in these rocks and although feldspars are a compositional solid solution between $CaAl_2Si_2O_8$, $NaAlSi_3O_8$ and $KAlSi_3O_8$, the variation in composition does not affect the ratio (in equivalents) of the product cation (Na^+, K^+, Ca^{2+}) to either the HCO_3^- or the SO_4^{2-} produced (cf. Eqns 5a, 5b, 6a and 6b). Analogous equations can be written for the main Mg-bearing silicate phases: illite ($(Al,Mg,Fe)_2(Si,Al)_4O_{10}OH_2$) and chlorite ($(Mg,Fe)_3(Si,Al)_4O_{10}$) (Table 4). In addition to mineral weathering, the oxidation of organic matter will produce HCO_3^-, and this reaction, which is expected to occur in these permafrost-dominated catchments, is represented by equation 7.
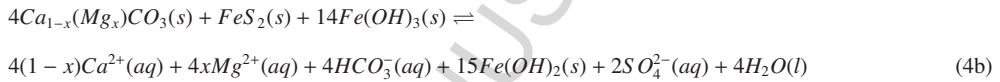
16

Carbonate dissolution with carbonic acid (CDC)
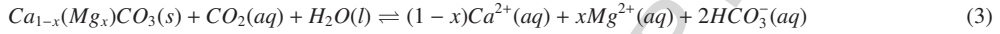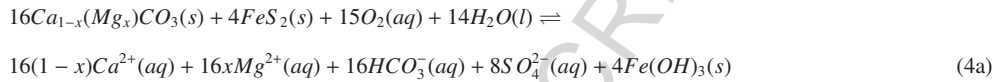
$$Ca_{1-x}(Mg_x)CO_3(s) + CO_2(aq) + H_2O(l) \rightleftharpoons (1-x)Ca^{2+}(aq) + xMg^{2+}(aq) + 2HCO_3^-(aq) \tag{3}$$

Aerobic sulfide oxidation coupled to carbonate dissolution (SOCD)

$$16Ca_{1-x}(Mg_x)CO_3(s) + 4FeS_2(s) + 15O_2(aq) + 14H_2O(l) \rightleftharpoons$$

$$16(1-x)Ca^{2+}(aq) + 16xMg^{2+}(aq) + 16HCO_3^-(aq) + 8SO_4^{2-}(aq) + 4Fe(OH)_3(s) \tag{4a}$$

Anaerobic sulfide oxidation coupled to carbonate dissolution (SOCD)

$$4Ca_{1-x}(Mg_x)CO_3(s) + FeS_2(s) + 14Fe(OH)_3(s) \rightleftharpoons$$

$$4(1-x)Ca^{2+}(aq) + 4xMg^{2+}(aq) + 4HCO_3^-(aq) + 15Fe(OH)_2(s) + 2SO_4^{2-}(aq) + 4H_2O(l) \tag{4b}$$

Silicate dissolution with carbonic acid, divalent cation (SDC)

$$2CaAl_2Si_2O_8(s) + 4CO_2(aq) + 6H_2O(l) \rightleftharpoons$$

$$2Ca^{2+}(aq) + 4HCO_3^-(aq) + Al_4Si_4O_{10}(OH)_8(s) \tag{5a}$$

Silicate dissolution with carbonic acid, monovalent cation (SDC)

$$2NaAlSi_3O_8(s) + 2CO_2(aq) + 11H_2O(l) \rightleftharpoons$$

$$2Na^+(aq) + 2HCO_3^-(aq) + Al_2Si_2O_5(OH)_4(s) + 4H_4SiO_4 \tag{5b}$$
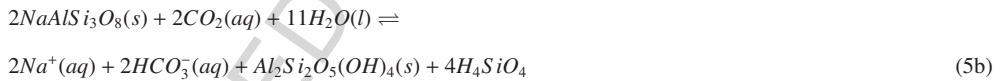
Sulfide oxidation coupled to silicate dissolution, divalent cation (SOSD)

$$2CaAl_2Si_2O_8(s) + FeS_2(aq) + \frac{15}{2}O_2(aq) + \frac{11}{2}H_2O(l) \rightleftharpoons$$

$$2Ca^{2+}(aq) + 2SO_4^{2-}(aq) + Al_4Si_4O_{10}(OH)_8(s) + Fe(OH)_3(s) \tag{6a}$$
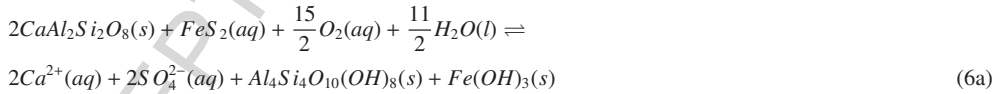
Sulfide oxidation coupled to silicate dissolution, monovalent cation (SOSD)

$$16NaSi_3O_8(s) + 4FeS_2(aq) + 15O_2(aq) + 86H_2O(l) \rightleftharpoons$$

$$16Na^+(aq) + 8SO_4^{2-}(aq) + 4Al_4Si_4O_{10}(OH)_8(s) + 4Fe(OH)_3(s) + 32H_4SiO_4(aq) \tag{6b}$$
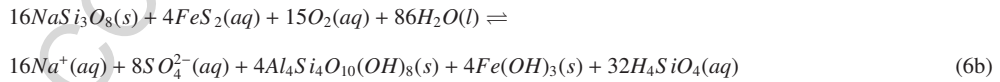
Organic matter oxidation (OMO)

$$CH_2O + O_2 \rightleftharpoons CO_2 + H_2O \rightleftharpoons HCO_3^- + H^+ \tag{7}$$

In the unglaciated catchment, Fardalen, the slope of the data in a plot of total cations versus SO_4^{2-} (Fig. 6a) is 1.04±0.04 which is the same as the slope which would be expected by sulfide oxidation coupled to silicate weathering (SOSD, Eqn. 6). The intercept of this line is not zero which suggests that a portion of the cations are being produced by other weathering reactions such as silicate dissolution by carbonic acid (SDC, Eqn. 5). In Figs. 6b and 6d, the slopes greater than 1 (carbonic acid weathering of silicates and carbonates, Table 6), together with the greater scatter of the Fardalen points support the notion that sulfuric acid is the main weathering agent in this catchment. In summary, although it is not possible to quantify the relative importance of each of the reactions represented by equations 3 -

Table 6: Predicted and observed slopes of Ca+Mg and total cations versus either SO_4^{2-} or HCO_3^-.

Reaction	Predicted slope (in eq)			
	$Ca^{2+}+Mg^{2+}$ vs SO_4^{2-}	$Ca^{2+}+Mg^{2+}$ vs HCO_3^-	Total Cations vs SO_4^{2-}	Total Cations vs HCO_3^-
Carbonate + H_2CO_3 (Eqn. 3)	∞	1	-	-
Carbonate + H_2SO_4 (Eqn. 4a,b)	2	2	-	-
Silicate + H_2CO_3 (Eqn. 5a,b)	-	-	∞	1
Silicate + H_2SO_4 (Eqn. 6a,b)	-	-	1	∞
	Observed slope			
Dryadbreen	1.54±0.14	1.48±0.29	1.84±0.18	2.04±0.42
Fardalen	0.88±0.04	6.68±2.10	1.04±0.04	7.92±2.50

7, the data from Fardalen is consistent with weathering mainly by a sulfide oxidation coupled to silicate dissolution process.

If only silicate minerals were weathering in the glaciated catchment (Dryadbreen) then the slopes of the data in Figs. 6a and 6b, which lie intermediate between SOSD (Eqn. 6) and SDC (Eqn. 5), would suggest that silicates are weathered by both carbonic and sulfuric acid. However, if it were assumed that all the Ca and Mg came from carbonates then the data points would also be consistent with carbonate weathering by sulfuric and carbonic acids (Figs. 6c and 6d). In summary, the data from Dryadbreen suggests that all four reactions are occurring i.e. weathering of both silicates and carbonates by both carbonic and sulfuric acid and further data from, for example, δ^{13}C-DIC and ^{87}Sr/^{86}Sr, would be needed to constrain the relative proportions of the different reactions.

The high proportion of silicate weathering in the unglaciated catchment is likely due to the presence of the active layer (the seasonally thawed top layer of soil above permafrost). If, over a long enough period, the active layer has remained at a constant depth, this would mean that despite frost-shattering exposing fresh mineral surfaces, the vast majority of carbonate phases will have already been leached, leaving behind the silicate minerals to weather. This is in agreement with the lack of carbonate detected by XRD in the orientated clay fractions of solid samples from Fardalen (Section 4.2). However, if the active layer deepens through a warming climate then fresh carbonates could become exposed (Keller et al., 2010). In contrast, high rates of physical erosion still occur in the glaciated catchment exposing carbonates to chemical weathering.

The nature of the weathering reactions in the glaciated catchment is in agreement with the conclusions of Tranter et al. (2002) who identified sulfide oxidation and Fe(III) reduction as key reactions in subglacial environments. The importance of sulfide oxidation reactions is also apparent in high-latitude unglaciated, permafrost dominated catchments (Fig. 6). This is in contrast to low-latitude, unglaciated catchments where weathering reactions are mainly driven by reaction with CO_2 either from respiration or from the atmosphere (Tranter et al., 2002).

Although the information in Fig. 6 provides an overview of the weathering reactions occurring in each catchment, further processes may modify these broad interpretations. Firstly, it is assumed that reactions have idealised stoichiometry and secondly, reactions removing solutes are not considered. The latter point is especially critical in subglacial environments where carbonate precipitation and sulfate reduction can occur (Wadham et al., 2004). Carbonate precipitation would decrease Ca^{2+} and HCO_3^-, whereas sulfate reduction would decrease SO_4^{2-}. All water

18

samples were undersaturated with respect to calcite and we therefore assume that carbonate precipitation did not have a significant impact on the stream water chemistry. In the following section we utilise the fact that the isotopes of sulfate (δ^{34}S and $\delta^{18}O_{SO4}$) are fractionated during reduction and can therefore be used to assess whether sulfate reduction is occurring and under what conditions.

5.2. Oxic or anoxic weathering conditions?

Sulfate reduction only occurs under anoxic conditions and previous studies have distinguished between aerobic and anaerobic environments based on the source of O atoms in sulfate (e.g. Bottrell and Tranter, 2002; Wadham et al., 2004). There are two main sources of oxygen: atmospheric O_2 and aqueous oxygen (H_2O) and each has a distinct isotopic composition.

During the oxidation of sulfide to sulfate the exchange of oxygen atoms in the intermediate molecules is very rapid but once sulfate has formed then exchange is negligible (Lloyd, 1968). Previously it has been assumed that if more than 75% of the O atoms in sulfate derive from water then the pyrite was oxidised under anoxic conditions and less than 75% implied oxidation under oxic conditions (Taylor et al., 1984; van Everdingen and Krouse, 1985). The fraction of O atoms in sulfate derived from atmospheric O_2 or water can be calculated as follows (Balci et al., 2007):

$$\delta^{18}O*_{SO4} = x(\delta^{18}O_{H2O} + \varepsilon^{18}O_{SO4\text{-}H2O}) + (1 - x)(\delta^{18}O_{O2} + \varepsilon^{18}O_{SO4\text{-}O2}) \qquad (8)$$

where x is the fraction of O atoms derived from H_2O and ε are the fractionation factors. When this principle was applied to glaciated catchments it was found that FeS_2 oxidation in subglacial environments proceeded primarily under anoxic conditions (Bottrell and Tranter, 2002; Wadham et al., 2004; Wynn et al., 2006; Wadham et al., 2007). However, recent studies have questioned the utility of $\delta^{18}O_{SO4}$ isotopes in distinguishing between oxic and anoxic conditions. These studies (Usher et al., 2004, 2005; Chandra and Gerson, 2011) found that even in solutions containing dissolved O_2 the vast majority of the oxygen atoms in sulfate derive from water because water outcompetes O_2 for adsorption sites. The percentage of oxygen atoms derived from water can therefore not be used to assess whether anoxic conditions are present or not during the oxidation of sulfide.

The bacterial sequencing data can, however, be used to gain a rough idea of the redox status of the two catchments. The samples from Dryadbreen were collected in summer whilst those from Fardalen were collected in spring and therefore may not be directly comparable as a result of seasonal variation in the microbial community composition (Crump et al., 2009; Schostag et al., 2015). However, a study on seasonal variations in the microbial community composition in soils found that the relative abundance of most phyla was constant over a year (Schostag et al., 2015). In addition, Arctic stream microbial community compositions were found to be strongly correlated with inorganic stream water chemistry (Crump et al., 2009) and given that there is more variation in relative ion proportions between the catchments than between the seasons (Fig. 6), we assume limited seasonal variability in the microbial community compositions for the purposes of this discussion.

19

Table 7: Abundance (%) of bacteria associated with Fe and S cycling. Sites A and O are from Dryadbreen and site L and M are from Fardalen.

Phylum/Class	Order	Genera	A	O	L	M
Reduces Fe(III)						
Acidobacteria	Holophagales	Geothrix	1.9	0.4	0.5	7.9
Betaproteobacteria	Burkholderiales	Albidiferax	0.6	1.1	0.2	1.3
Betaproteobacteria	Burkholderiales	Rhodoferax ferrireducens	2.9	4.1	0.4	1.3
Deltaproteobacteria	Desulfuromonadales	Geobacter	8.1	1.8	0.0	3.9
Oxidizes Fe(II)						
Betaproteobacteria	Ferritrophicales	Ferritrophicum radicicola	0.5	0.0	0.0	0.0
Betaproteobacteria	Gallionellales	Sideroxydans lithotrophicus	0.6	1.1	3.4	0.1
Betaproteobacteria	Hydrogenophilales	Thiobacillus	5.9	0.1	2.9	0.8
Oxidizes reduced S compounds						
Betaproteobacteria	Burkholderiales	Thiobacter subterraneus	0.0	0.1	0.8	0.0
Betaproteobacteria	Hydrogenophilales	Sulfuricella	0.9	0.0	0.8	0.4
Betaproteobacteria	Hydrogenophilales	Thiobacillus	5.9	0.1	2.9	0.8
Gammaproteobacteria	Chromatiales	Halothiobacillus neapolitanus	0.0	0.0	0.5	0.0
Gammaproteobacteria	Chromatiales	Thioalkalivibrio versutus	0.0	0.0	0.1	0.0
Gammaproteobacteria	Chromatiales	Thiocapsa machilipatnamensis	0.0	0.0	0.5	0.0
Reduces sulfate						
Deltaproteobacteria	Desulfobacterales	Desulfatiferula	0.0	0.1	0.0	0.0
Deltaproteobacteria	Desulfobacterales	Desulfobulbus	0.0	0.0	0.0	0.1
Deltaproteobacteria	Desulfobacterales	unclassified	0.1	0.4	0.0	0.4
Firmicutes	Clostridiales	Desulfosporosinus	0.3	0.6	0.0	5.2

Some bacteria only live in anaerobic environments and therefore their presence can be used as an indication that anoxic conditions are present. In both catchments, we found evidence for both anaerobic and aerobic bacteria in the under-water sites (A and L) suggesting that anoxic micro-niches exist in the aqueous system. Sequences affiliated with *Thiobacillus*, a facultative aerobe capable of oxidizing iron and sulfur compounds was represented in both catchments (Table 7). It is likely that *Thiobacillus* is involved in the aerobic oxidation of pyrite and as a result may help establish anoxic conditions. However, the Deltaproteobacteria class of bacteria, which consists of numerous lithotrophic anaerobes (Kuever et al., 2005), was strongly represented in Dryadbreen (glaciated, Site A, 10.3%) but was nearly absent in Fardalen (unglaciated, Site L, 0.1%) (Fig. 5), suggesting that anoxic conditions may be more prevalent in the glaciated catchment and that iron reduction may be an important process. In support of this notion, a number of genera capable of reducing iron compounds were identified (Table 7). For example, 8.1% and 2.9% of the sequences from Dryadbreen (A) were closely affiliated with *Geobacter* (obligate anaerobe, Lovley, 2000) and *Rhodoferax* (facultative anaerobe, Finneran et al., 2003) respectively (Table 7). Anoxia may be more prevalent in the glaciated catchment due to the sandur, which is a large wet area covered by fine glacial flour, conditions which would favour pyrite oxidation and the development of anoxia, analogous to marine sediments (e.g. Burdige, 1993). Additionally, the sandur is underlain by ice (Ziaja and Pipała, 2007) which could be hydraulically linked to the subglacial drainage system providing a pathway for anoxic subglacial meltwater to enter the stream downstream of the apparent glacier front (Irvine-Fynn et al., 2011). In the unglaciated catchment, the aforementioned processes are not relevant. Although the deeper permafrost areas will be anoxic, they may not have a strong hydraulic connection to the stream, resulting in a stream which is dominantly oxic.

5.3. Sulfur isotope fractionation: oxidation or reduction?

Sulfate reduction only occurs in anaerobic environments and in low-temperature natural systems it is biologically mediated (Seal II, 2006). During sulfate reduction both $\delta^{34}S$ and $\delta^{18}O_{SO4}$ values in the remaining SO_4 will increase as the light isotope is the preferred reactant. A positive correlation between $\delta^{34}S$ and $\delta^{18}O_{SO4}$ has therefore been proposed as diagnostic of sulfate reduction (e.g. Mandernack et al., 2003).

The spring $\delta^{34}S$ values from both catchments have similar $\delta^{34}S$ values that are within error of one of the measured pyrite mineral separates suggesting that no sulfate reduction has occurred (Fig. 7). The summer $\delta^{34}S$ values from Fardalen are about 3‰ lighter in $\delta^{34}S$ compared to the spring points but have the same isotopic composition as one of the measured pyrite mineral separates, again suggesting the absence of sulfate reduction. The apparent shift in the inferred source pyrite $\delta^{34}S$ value could be due to differences in pyrite $\delta^{34}S$ values between the different formations (Table 5): waters in spring could predominantly drain the Frysjaodden Formation whereas waters in summer could access formations higher up in the catchment (e.g. Battfjellet) as the snow pack retreats. However, the summer $\delta^{34}S$ values from Dryadbreen are heavier in $\delta^{34}S$ compared to both measured and inferred pyrite compositions and, additionally, there is also a significant positive correlation between $\Delta^{18}O_{SO4-H2O}$ and $\delta^{34}S$ ($R^2=0.99$, p<0.001, m=6±1) which is suggestive of sulfate reduction (Mandernack et al., 2003; Turchyn et al., 2013). $\Delta^{18}O_{SO4-H2O}$ is used instead of $\delta^{18}O_{SO4}$ in order to remove the effect on $\delta^{18}O_{SO4}$ of the temporal variation in $\delta^{18}O_{H2O}$. The gradient of the slope between $\delta^{18}O_{SO4}$ and $\delta^{34}S$ is thought to give information on reaction pathways. Oxygen isotope variations during reduction are thought to be controlled by a combination of intra-cellular isotope exchange between intermediate sulfur compounds and ambient water (Brunner et al., 2005; Farquhar et al., 2008) and kinetic fractionation at the cell level (Aharon and Fu, 2000; Mandernack et al., 2003). The balance between exchange and kinetic isotope fractionation is dependent on the overall reaction rate. Thus, the exact slope of $\delta^{18}O_{SO4}$ versus $\delta^{34}S$ depends on which microbial species mediate the reaction and the forward and backward reaction rates (Aharon and Fu, 2000; Mandernack et al., 2003; Kleikemper et al., 2004; Turchyn et al., 2010; Wankel et al., 2014). The slope of $\Delta^{18}O_{SO4-H2O}$ versus $\delta^{34}S$ from Fig. 7 is 6 which would indicate a slow reaction rate (Brunner et al., 2005).

However, if significant sulfate reduction was occurring in Dryadbreen then appreciable amounts of sulfate reducing bacteria would have been expected to be detected using molecular analysis. In the sediment sample (A), only 0.4% of the bacteria were inferred to have the capacity to reduce sulfate. In addition, attempts to amplify the gene encoding a fragment of the alpha and beta subunit of the bisulphate reductase (*dsrAB*, a biomarker for sulfate reduction, Wagner et al., 1998) were not successful in any of the four sediment samples despite 40 cycles of PCR (data not shown). This supports the notion that the observed sulfur isotope fractionation was not due to sulfate reduction.

It is generally assumed that negligible sulfur isotope fractionation occurs during pyrite oxidation, however fractionation can occur under certain conditions. Several biotic and abiotic experiments under anoxic and oxic conditions have observed $\varepsilon_{SO4-pyrite}$ with values between -1.3 and +3.5‰ (Balci et al., 2007; Pisapia et al., 2007; Brunner et al., 2008). The difference between pyrite and sulfate in the Dryadbreen summer samples is $\Delta^{34}S_{SO4-sulfide} = +2.2$ to +4.8‰, depending on which value for $\delta^{34}S_{sulfide}$ is used (Table 5). Positive values, of similar magnitude ($\varepsilon_{SO4-sulfide}$

21

= +3.5 and +0.4) have previously been reported for the initial, non-stoichiometric stages of pyrite oxidation (Pisapia et al., 2007; Brunner et al., 2008). Non-stoichiometric reactions are expected to occur in areas of significant physical erosion e.g. glaciated catchments, as material is removed before reactions are completed (kinetic limitation, Stallard and Edmond, 1983). Positive values of $\varepsilon_{SO4-sulfide}$ have been attributed to heightened loss of SO_2 in the early stages of the reaction and the breaking of thiosulfate S-S covalent bonds (Pisapia et al., 2007; Brunner et al., 2008). Degassing of SO_2 is likely under acidic conditions, but the pH of this river is around 6.5 (Table 1), suggesting that this mechanism of fractionation is likely to be minor. Similarly, the fractionation of O isotopes in sulfate can occur when sulfite species are present, allowing oxygen isotope exchange with water, enriching sulfite, and ultimately sulfate, with ^{18}O (Brunner et al., 2008). The $\Delta^{18}O_{SO4-water}$ values from Dryadbreen summer samples (+3.0 to +5.4‰) are in agreement with $\varepsilon^{18}O_{SO4-water}$ data from pyrite oxidation experiments (+2.8 to +16‰, Balci et al., 2007; Pisapia et al., 2007; Brunner et al., 2008). In conclusion, sulfate enriched in both ^{34}S and ^{18}O, as observed in Dryadbreen, does not necessarily imply sulfate reduction and can be adequately explained as a result of non-stoichiometric reaction pathways during the oxidation of pyrite.

In Dryadbreen (site A) 21.7% of the bacteria (collected in summer) are inferred to be involved in Fe and S cycling reactions and 13.5% are inferred to have the ability to reduce Fe(III) e.g. *Geobacter* and *Rhodoferax* (Table 7). Given that pyrite is likely the main source of iron in the system, the obligate anaerobic nature of *Geobacter* and the facultative anaerobic nature of *Rhodoferax*, are suggestive of the presence and potential importance of anoxic portions of the catchment where the 'anoxic' pyrite oxidation pathway may occur (Eqn 4b, note that this pathway can also occur where oxygen is present e.g. Balci et al. (2007)). The pH of the water is circumneutral, likely due to the buffering capacity of calcite dissolution, and at this pH Fe can be cyclically oxidised and reduced (Moses and Herman, 1991) accounting for the presence of bacteria associated with both Fe reduction and Fe oxidation. It is also possible for other compounds to act as the electron acceptor in pyrite reduction such as NO_3 and MnO_2, and it is likely that all will be involved in pyrite oxidation to some extent if they are available in the system (e.g. Burdige and Nealson, 1986; Jørgensen et al., 2009). Indeed, an abundant component of the microbial community identified at Site A (Dryadbreen) is *Thiobacillus* (Table 7) which can couple FeS_2 oxidation with NO_3^- reduction (Bosch et al., 2012). Therefore, the presence of the above-mentioned bacteria indicates that the non-stoichiometric reaction pathway, identified as being responsible for the observed change in δ^{34}S and $\delta^{18}O_{SO4}$ values, most likely occurs under anoxic conditions and involves the reduction of Fe. In Fardalen (site L) the bacteria involved in Fe and S cycling are associated with oxidation of Fe and reduced S compounds, with a much lower fraction ($\sim 1\%$) inferred to be involved in Fe reduction. This corroborates the inference of pyrite oxidation under oxic conditions and isotopic fractionation of S and O in sulfate is not observed due to the complete conversion of sulfide to sulfate (Seal II, 2006).

6. Wider implications

The isotopic and concentration data suggest that in the unglaciated catchment, mineral dissolution occurs mainly by reaction with sulfuric acid. In the glaciated catchment the balance between sulfuric acid and carbonic acid is more even, but due to the non-stoichiometric conversion of pyrite to sulfate (loss of intermediate S compounds) as indicated by the stable isotope data, weathering by sulfuric acid may be underestimated. This indicates that sulfuric acid weathering is not only important in glaciated catchments (e.g. Wadham et al., 2010) but also in permafrost dominated catchments (Nowak and Hodson, 2015) and could therefore be a widespread phenomenon throughout the permafrost zone where shale exists (approximately 46% of the land draining into the Arctic ocean, Amiotte Suchet et al., 2003). Indeed, data from the Mackenzie river, the fourth largest Arctic river by discharge and with extensive shale and permafrost areas, demonstrates the significant contribution of sulfuric acid weathering (Calmels et al., 2007). Quantification of the contribution of sulfuric acid weathering on a global scale is necessary because, if significant, it weakens the climate-weathering negative feedback because if allows cations to be released without accompanying bicarbonate in the case of silicates and the release of bicarbonate without uptake of atmospheric CO_2 in the case of carbonates (Calmels et al., 2007; Li et al., 2008; Torres et al., 2014).

7. Conclusions

The presence of a glacier appeared to alter both the bacterial community composition and chemical weathering reactions in a sedimentary catchment containing pyrite in Svalbard, compared to a neighbouring unglaciated catchment. The dominant anion in the unglaciated catchment was SO_4^{2-} whereas in the glaciated catchment the dominant anion was HCO_3^-. The difference in major anion composition was attributed to differences in the chemical weathering reactions occurring in both catchments: silicate weathering by sulfuric acid in the unglaciated catchment and carbonate and silicate weathering by carbonic and sulfuric acids in the glaciated catchment. We speculate that the high erosion rates in the glaciated catchment continually expose carbonate minerals whereas carbonate has already been leached from the permafrost active layer in the unglaciated catchment.

Sulfide oxidation was a key process generating acidity in both catchments but this reaction appeared to occur by different mechanisms in each catchment. In the unglaciated catchment, $\delta^{34}S$ values of stream water were identical to those measured in pyrite and, together with the bacterial community composition, this suggested that pyrite oxidation occurred under oxic conditions. A seasonal shift in the absolute $\delta^{34}S$ value of stream water was attributed to the draining of different sedimentary formations. In the glaciated catchment, the summer $\delta^{34}S$ values were positively correlated to $\delta^{18}O_{SO4}$, suggesting sulfate reduction. However, this process is microbially mediated and a biomarker for sulfate reduction (*dsrAB* genes) was not detected in stream sediments. Instead, the bacterial composition is consistent with fractionation due to sulfide oxidation under anoxic conditions with loss of sulfur intermediates, inducing isotopic fractionation in S between sulfide and sulfate. The presence of bacteria associated with iron redox cycling suggests the involvement of Fe^{3+} as an electron acceptor in this environment.

23

As the local environment changes due to deglaciation and permafrost thaw, the bacterial community is expected to change in response. As a result, microbial mediated reactions, such as those involving sulfur compounds, will be affected. Thus, changes in the solute composition of streams can be expected as a result of continued warming in the Arctic.

8. Acknowledgments

9. References

Aharon, P., Fu, B., 2000. Microbial sulfate reduction rates and sulfur and oxygen isotope fractionations at oil and gas seeps in deepwater Gulf of Mexico. Geochim. Cosmochim. Acta 64, 233–246.

Amiotte Suchet, P., Probst, J. L., Ludwig, W., 2003. Worldwide distribution of continental rock lithology: Implications for the atmospheric/soil CO_2 uptake by continental weathering and alkalinity river transport to the oceans. Global Biogeochem. Cycles 17, 1038.

Balci, N., Shanks III, W. C., Mayer, B., Mandernack, K. W., 2007. Oxygen and sulfur isotope systematics of sulfate produced by bacterial and abiotic oxidation of pyrite. Geochim. Cosmochim. Acta 71, 3796–3811.

Berner, K. E., Berner, R. A., 1996. Global environment: Water, air and geochemical cycles. Prentice-Hall, Upper Saddle River, N.J.

Bosch, J., Lee, K. Y., Jordan, G., Kim, K. W., Meckenstock, R. U., 2012. Anaerobic, nitrate-dependent oxidation of pyrite nanoparticles by *thiobacillus denitrificans*. Environ. Sci. Technol. 46, 2095–2101.

Bottrell, S. H., Tranter, M., 2002. Sulphide oxidation under partially anoxic conditions at the bed of the Haut Glacier d'Arolla, Switzerland. Hydrol. Process. 16, 2363–2368.

Boyd, E. S., Hamilton, T. L., Havig, J. R., Skidmore, M. L., Shock, E. L., 2014. Chemolithotrophic primary production in a subglacial ecosystem. Appl. Environ. Microbiol. 80, 6146–6153.

Boyd, E. S., Jackson, R. A., Encarnacion, G., Zahn, J. A., Beard, T., Leavitt, W. D., Pi, Y., Zhang, C. L., Pearson, A., Geesey, G. G., 2007. Geothermal springs in yellowstone acid-sulfate-chloride-containing sulfur-respiring crenarchaea inhabiting isolation, characterization, and ecology of sulfur-respiring *Crenarchaea* inhabiting acid-sulfate-chloride-containing geothermal springs in Yellowstone National Park. Appl. Environ. Microbiol. 73, 6669–6677.

537 Boyd, E. S., Lange, R. K., Mitchell, A. C., Havig, J. R., Hamilton, T. L., Lafrenière, M. J., Shock, E. L., Peters, J. W., Skidmore, M., 2011.
538 Diversity, abundance, and potential activity of nitrifying and nitrate-reducing microbial assemblages in a subglacial ecosystem. Appl. Environ.
539 Microbiol. 77, 4778–4787.

540 Brunner, B., Bernasconi, S. M., Kleikemper, J., Schroth, M. H., 2005. A model for oxygen and sulfur isotope fractionation in sulfate during
541 bacterial sulfate reduction processes. Geochim. Cosmochim. Acta 69, 4773–4785.

542 Brunner, B., Yu, J. Y., Mielke, R. E., MacAskill, J. A., Madzunkov, S. amd McGenity, T. J., Coleman, M., 2008. Different isotope and chemical
543 patterns of pyrite oxidation related to lag and exponential growth phases of *Acidithiobacillus ferrooxidans* reveal a microbial growth strategy.
544 Earth Planet. Sci. Lett. 270, 63–72.

545 Burdige, D. J., 1993. The biogeochemistry of manganese and iron reduction in marine sediments. Earth Sci. Rev. 35, 249–284.

546 Burdige, D. J., Nealson, K. H., 1986. Chemical and microbiological studies of sulfide-mediated manganese reduction. Geomicrobiol. J. 4, 361–387.

547 Calmels, D., Gaillardet, J., France-Lanord, C., 2007. Sustained sulfide oxidation by physical erosion processes in the Mackenzie River basin:
548 Climatic perspectives. Geology 35, 1003–1006.

549 Chandra, A. P., Gerson, A. R., 2011. Pyrite (FeS_2) oxidation: A sub-micron synchrotron investigation of the initial steps. Geochim. Cosmochim.
550 Acta 75, 6239–6254.

551 Crump, B. C., Peterson, B. J., Raymond, P. A., Amon, R. M. W., Rinehart, A., McClelland, J. W., Holmes, R. M., 2009. Circumpolar synchrony in
552 big river bacterioplankton. P. Natl. Acad. Sci. 106, 21208–21212.

553 Darriba, D., Taboada, G. L., Doalla, R., Posada, D., 2012. jModelTest 2: more models, new heuristics and parallel computing. Nat. Meth. 9, 772.

554 Dypvik, H., Riber, L., Burca, F., Rüther, D., Jargvoll, D., Nagy, J., Jochmann, M., 2011. The Paleocene-Eocene thermal maximum (PETM) in
555 Svalbard - clay mineral and geochemical signals. Palaeogeogr. Palaeoclimatol. Palaeoecol. 302, 156–169.

556 Edgar, R. C., Haas, B. J., Clemente, J. C., Quince, C., Knight, R., 2011. UCHIME improves sensitivity and speed of chimera detection. Bioinfor-
557 matics 27, 2194–2200.

558 Elberling, B., Langdahl, B. R., 1998. Natural heavy-metal release by sulphide oxidation in the High Arctic. Can. Geotech. J. 35, 895–901.

559 Elberling, B., Michelsen, A., Schädel, C., Schuur, E. A. G., Christiansen, H. H., Berg, L., Tamstorf, M. P., Sigsgaard, C., 2013. Long-term CO_2
560 production following permafrost thaw. Nat. Clim. Change 3, 890–894.

561 Etzelmüller, B., Hagen, J. O., 2005. Glacier-permafrost interaction in Arctic and alpine mountain environments with examples from southern
562 Norway and Svalbard. In: Harris, C., Murton, J. B. (Eds.), Cryospheric systems: Glaciers and Permafrost. Vol. 242 of Special Publications.
563 Geological Society, London, pp. 11–27.

564 Etzelmüller, B., Ødegård, R. S., Vatne, G., Mysterud, R. S., Tonning, T., Sollid, J. L., 2000. Glacier characteristics and sediment transfer system of
565 Longyearbreen and Larsbreen, western Spitsbergen. Norsk Geografisk Tidskrift 54, 157–168.

566 Fairchild, I. J., Bradby, L., Sharp, M., Tison, J.-L., 1994. Hydrochemistry of carbonate terrains in alpine glacial settings. Earth Surf. Process.
567 Landforms 19, 33–54.

568 Fairchild, I. J., Killawee, J. A., Hubbard, B., Dreybrodt, W., 1999. Interactions of calcareous suspended sediment with glacial meltwater: a field
569 test of dissolution behaviour. Chem. Geol. 155, 243–263.

570 Farquhar, J., Canfield, D. E., Masterson, A., Bao, H., Johnston, D., 2008. Sulfur and oxygen isotope study of sulfate reduction in experiments with
571 natural populations from Fællestrand, Denmark. Geochim. Cosmochim. Acta 72, 2805–2821.

572 Finneran, K. T., Johnson, C. V., Lovley, D. R., 2003. *Rhodoferax ferrireducens* sp. nov., a psychrotolerant, facultatively anaerobic bacterium that
573 oxidises acetate with the reduction of Fe(III). Int. J. Syst. Evol. Microbiol. 53, 669–673.

574 Foght, J., Aislabie, J., Turner, S., Brown, C. E., Ryburn, J., Saul, D. J., Lawson, W., 2004. Culturable bacteria in subglacial sediments and ice from
575 two southern hemisphere glaciers. Microbial Ecology 47, 329–340.

576 Frey, K. E., McClelland, J. W., 2009. Impacts of permafrost degradation on arctic river biogeochemistry. Hydrol. Process. 23, 169–182.

577 Grasby, S. E., Allen, C. C., Longazo, T. G., Lisle, J. T., Griffin, D. W., Beauchamp, B., 2003. Supraglacial sulfur springs and associated biological
578 activity in the Canadian High Arctic - signs of life beneath the ice. Astrobiology 3, 583–596.

579 Guindon, S., Gascuel, O., 2003. A simple, fast, and accurate algorithm to estimate large phylogenies by maximum likelihood. Syst. Biol. 52,

25

696–704.

Hall, K., Thorn, C. E., Matsuoka, N., Prick, A., 2002. Weathering in cold regions: some thought and perspectives. Prog. Phys. Geog. 26, 577–602.

Hammer, Ø., Harper, D. A. T., Ryan, P. D., 2001. PAST: Paleontological statistics software package for education and data analysis. Palaeontol. Electronica 4, 1–9.

Havig, J. R., Raymond, J., Meyer-Dombard, D. R., Zolotova, N., Shock, E. L., 2011. Merging isotopes and community genomics in a siliceous sinter-depositing hot spring. J. Geophys. Res. 116, G01005.

Herron, M. M., 1988. Geochemical classification of terrigenous sands and shales from core or log data. J. Sediment. Petrol. 58, 820–829.

Hindshaw, R. S., Tipper, E. T., Reynolds, B. C., Lemarchand, E., Wiederhold, J. G., Magnusson, J., Bernasconi, S. M., Kretzschmar, R., Bourdon, B., 2011. Hydrological control of stream water chemistry in a glacial catchment (Damma Glacier, Switzerland). Chem. Geol. 285, 215–230.

Hodgkins, R., Tranter, M., Dowdeswell, J. A., 1997. Solute provenance, transport and denudation in a high arctic glacierized catchment. Hydrol. Process. 11, 1813–1832.

Hodson, A., Anesio, A. M., Tranter, M., Fountain, A., Osborn, M., Priscu, J., Laybourn-Parry, J., Sattler, B., 2008. Glacial ecosystems. Ecol. Monogr. 78, 41–67.

Holland, H. D., 1978. The chemistry of the atmosphere and oceans. Wiley-Interscience, New York.

Hudson, R., Fraser, J., 2005. Introduction to salt dilution gauging for streamflow measurement Part IV: The mass balance (or dry injection) method. Streamline Watershed Management Bulletin 9, 6–12.

Huh, Y., Edmond, J. M., 1999. The fluvial geochemistry of the rivers of Eastern Siberia: III. Tributaries of the Lena and Anabar draining the basement terrain of the Siberian Craton and the Trans-Baikal Highlands. Geochim. Cosmochim. Acta 63, 967–987.

Humlum, O., Instanes, A., Sollid, J. L., 2003. Permafrost in Svalbard: a review of research history, climatic background and engineering challenges. Polar Res. 22, 191–215.

Irvine-Fynn, T. D. L., Hodson, A. J., Moorman, B. J., Vatne, G., Hubbard, A. L., 2011. Polythermal glacier hydrology: a review. Reviews of Geophysics 49, 1–37.

Johannessen, M., Henriksen, A., 1978. Chemistry of snow meltwater: changes in concentration during melting. Water Resour. Res. 14, 615–619.

Jørgensen, C. J., Jacobsen, O. S., Elberling, B., Aamand, J., 2009. Microbial oxidation of pyrite coupled to nitrate reduction in anoxic groundwater sediment. Environ. Sci. Technol. 43, 4851–4857.

Keller, K., Blum, J. D., Kling, G. W., 2010. Stream geochemistry as an indicator of increasing permafrost thaw depth in an arctic watershed. Chem. Geol. 273, 76–81.

Kendall, C., Doctor, D. H., 2003. Stable isotope applications in hydrologic studies. In: Holland, H. D., Turekian, K. K. (Eds.), Treatise on Geochemistry. Vol. 5. Surface and groundwater, weathering, and soils. Elsevier, pp. 319–364.

Kleikemper, J., Schroth, M. H., Bernasconi, S. M., Brunner, B., Zeyer, J., 2004. Sulfur isotope fractionation during growth of sulfate-reducing bacteria on various carbon sources. Geochim. Cosmochim. Acta 68, 4891–4904.

Kuever, J., Rainey, F. A., Widdel, F., 2005. Class IV. Deltaproteobacteria class nov. In: Garrity, G., Brenner, D. J., Krieg, N. R., Staley, J. T. (Eds.), Bergey's Manual® of Systematic Bacteriology. Vol. 2: The Proteobacteria (Part C). Springer Verlag, pp. 922–1144.

Lafrenière, M. J., Sharp, M. J., 2005. A comparison of solute fluxes and sources from glacial and non-glacial catchments over contrasting melt seasons. Hydrol. Process. 19, 2991–3012.

Larkin, M. A., Blackshields, G., Brown, N. P., Chenna, R., McGettigan, P. A., McWilliam, H., Valentin, F., Wallace, I. M., Wilm, A., Lopez, R., Thompson, J. D., Gibson, T. J., Higgins, D. G., 2007. Clustal W and Clustal X version 2.0. Bioinformatics 23, 2947–2948.

Larouche, J. R., Bowden, W. B., Giordano, R., Flinn, M. B., Crump, B. C., 2012. Microbial biogeography of arctic streams: exploring influences of lithology and habitat. Front. Microbiol. 3, 309.

Li, S. L., Calmels, D., Han, G., Gaillardet, J., Liu, C. Q., 2008. Sulfuric acid as an agent of carbonate weathering constrained by $\delta^{13}C_{DIC}$: Examples from Southwest China. Earth Planet. Sci. Lett. 270, 189–199.

Lloyd, R. M., 1968. Oxygen isotope behavior in the sulfate-water system. J. Geophys. Res. 73, 6099–6110.

Lovley, D. R., 2000. Dissimilatory Fe(III)- and Mn(IV)-reducing prokaryotes. In: Dworkin, M., Falkow, S., Rosenberg, E., Stackebrandt, E. (Eds.),

The Prokaryotes. Springer, New York.

MacLean, R., Oswood, M. W., Irons III, J. G., McDowell, W. H., 1999. The effect of permafrost on stream biogeochemistry: A case study of two streams in the Alaskan (U.S.A.) taiga. Biogeochemistry 47, 239–267.

Major, H., Haremo, P., Dallmann, W. K., Andresen, A., 2000. Geological map of Svalbard 1:100 000, sheet C9G Adventdalen, Temakart nr. 31. Norsk Polarinstitutt, Tromsø, Norway.

Mandernack, K. W., Krouse, H. R., Skei, J. M., 2003. A stable sulfur and oxygen isotopic investigation of sulfur cycling in an anoxic marine basin, Framvaren Fjord, Norway. Chem. Geol. 195, 181–200.

Meuser, J, E., Baxter, B. K., Spear, J. R., Peters, J. W., Posewitz, M. C., Boyd, E. S., 2013. Contrasting patterns of community assembly in the stratified water column of Great Salt Lake, Utah. Microb. Ecol. 66, 268–280.

Mitchell, A. C., Lafrenière, M. J., Skidmore, M. L., Boyd, E. S., 2013. Influence of bedrock mineral composition on microbial diversity in a subglacial environment. Geology 41, 855–858.

Montross, S. N., Skidmore, M., Tranter, M., Kivimäki, A. L., Parkes, R. J., 2013. A microbial driver of chemical weathering in glaciated systems. Geology 41, 215–218.

Moses, C. O., Herman, J. S., 1991. Pyrite oxidation at circumneutral pH. Geochim. Cosmochim. Acta 55, 471–482.

Nowak, A., Hodson, A., 2015. On the biogeochemical response of a glacierized High Arctic watershed to climate change: revealing patterns, processes and heteogeneity among micro-catchments. Hydrol. Process. 29, 1588–1603.

Pisapia, C., Chaussidon, M., Mustin, C., Humbert, B., 2007. O and S isotopic composition of dissolved and attached oxidation products of pyrite by *Acidithiobacillus ferrooxidans*: Comparison with abiotic oxidations. Geochim. Cosmochim. Acta 71, 2474–2490.

Pokrovsky, O. S., Viers, J., Dupré, B., Chabaux, F., Gaillardet, J., Audry, S., Prokushkin, A. S., Shirokova, L. S., Kirpotin, S. N., Lapitsky, S. A., Shevchenko, V. P., 2012. Biogeochemistry of carbon, major and trace elements in watersheds of northern Eurasia drained to the Arctic Ocean: The change of fluxes, sources and mechanisms under the climate warming prospective. C. R. Geosci. 344, 663–677.

Rao, C. R., 1982. Diversity and dissimilarity coefficients: A unified approach. Theor. Popul. Biol. 21, 24–43.

Robinson, Z. P., Fairchild, I. J., Spiro, B., 2009. The sulphur isotope and hydrochemical characteristics of Skeiðarársandur, Iceland: identification of solute sources and implications for weathering processes. Hydrol. Process. 23, 2212–2224.

Schlegel, A., Lisker, F., Dörr, N., Jochmann, M., Schubert, K., Spiegel, C., 2013. Petrography and geochemistry of siliclastic rocks from the Central Tertiary Basin of Svalbard - implications for provenance, tectonic setting and climate. Z. Dt. Ges. Geowiss. 164, 173–186.

Schloss, P. D., Westcott, S. L., Ryabin, T., Hall, J. R., Hartmann, M., Hollister, E. B., Lesniewski, R. A., Oakley, B. B., Parks, D. H., Robinson, C. P., Sahl, J. W., Stres, B., Thallinger, G. G., Van Horn, D. J., Weber, C. F., 2009. Introducing mothur: open-source, platform-independent, community-supported software for describing and comparing microbial communities. Appl. Environ. Microbiol. 75, 7537–7541.

Schostag, M., Stibal, M., Jacobsen, C. S., Bælum, J., Taş, N., Elberling, B., Jansson, J. K., Semenchuk, P., Priemé, A., 2015. Distinct summer and winter bacterial communities in the active layer of Svalbard permafrost revealed by DNA-and RNA-based analyses. Front. Microbiol. 6, 399.

Schuur, E. A. G., Vogel, J. G., Crummer, K. G., Lee, H., Sickman, J. O., Osterkamp, T. E., 2009. The effect of permafrost thaw on old carbon release and net carbon exchange from tundra. Nature 459, 556–559.

Seal II, R. R., 2006. Sulfur isotope geochemistry of sulfide minerals. In: Vaughan, D. J. (Ed.), Sulfide mineralogy and geochemistry. Vol. 61 of Reviews in Mineralogy and Geochemistry. Mineralogical Society of America, pp. 633–677.

Sharp, M., Creaser, R. A., Skidmore, M., 2002. Strontium isotope composition of runoff from a glaciated carbonate terrain. Geochim. Cosmochim. Acta 66, 595–614.

Skidmore, M., Anderson, S. P., Sharp, M., Foght, J., Lanoil, B. D., 2005. Comparison of microbial community compositions of two subglacial environments reveals a possible role for microbes in chemical weathering processes. Appl. Environ. Microb. 71, 6986–6997.

Skidmore, M. L., Foght, J. M., Sharp, M. J., 2000. Microbial life beneth a High Arctic glacier. Appl. Environ. Microb. 66, 3214–3220.

Stallard, R. F., Edmond, J. M., 1983. Geochemistry of the Amazon 2. The influence of geology and weathering environment on the dissolved load. J. Geophys. Res. 88, 9671–9688.

Stumm, W., Morgan, J. J., 1996. Aquatic Chemistry: chemical equilibria and rates in natural waters, 3rd Edition. Wiley.

666 Svendsen, J. I., Mangerud, J., 1997. Holocene glacial and climatic variations on Spitsbergen, Svalbard. Holocene 7, 45–57.

667 Swofford, D. L., 2001. PAUP: Phylogenetic analysis using parsimony (and other methods). Sinauer Associate: Sunderland, MA, USA, 4.0b10 Edn.

668 Taylor, B. E., Wheeler, M. C., Nordstrom, D. K., 1984. Isotope composition of sulphate in acid mine drainage as measure of bacterial oxidation.

669   Nature 308, 538–541.

670 Thorn, C. E., Darmody, R. G., Dixon, J. C., Schlyter, P., 2001. The chemical weathering regime of Kärkevagge, arctic-alpine Sweden. Geomor-

671   phology 41, 37–52.

672 Torres, M. A., West, A. J., Li, G., 2014. Sulphide oxidation and carbonate dissolution as a source of co_2 over geological timescales. Nature.

673 Tranter, M., Sharp, M. J., Lamb, H. R., Brown, G. H., Hubbard, B. P., Willis, I. C., 2002. Geochemical weathering at the bed of Haut Glacier

674   d'Arolla, Switzerland - a new model. Hydrol. Process. 16, 959–993.

675 Turchyn, A. V., Brüchert, V., Lyons, W. B., Engel, G. S., Balci, N., Schrag, D. P., Brunner, B., 2010. Kinetic oxygen isotope effects during

676   dissimilatory sulfate reduction: A combined theoretical and experimental approach. Geochim. Cosmochim. Acta 74, 2011–2024.

677 Turchyn, A. V., Tipper, E. T., Galy, A., Lo, J. K., Bickle, M. J., 2013. Isotope evidence for secondary sulfide precipitation along the Marsyandi

678   River, Nepal, Himalayas. Earth Planet. Sci. Lett. 374, 36–46.

679 Tye, A. M., Heaton, T. H. E., 2007. Chemical and isotopic characteristics of weathering and nitrogen release in non-glacial drainage waters on

680   Arctic tundra. Geochim. Cosmochim. Acta 71, 4188–4205.

681 Usher, C. R., Cleveland, C. A., Strongin, D. R., Schoonen, M. A., 2004. Origin of oxygen in sulfate during pyrite oxidation with water and dissolved

682   oxygen: an in-situ horizontal attenuated total reflectance infrared spectroscpoy isotope study. Environ. Sci. Technol. 38, 5604–5606.

683 Usher, C. R., Paul, K. W., Narayansamy, J., Kubicki, J. D., Sparks, D. L., Schoonen, M. A., Strongin, D. R., 2005. Mechanistic aspects of pyrite

684   oxidation in an oxidizing gaseous environment: an in situ HATR-IR isotope study. Environ. Sci. Technol. 39, 7576–7584.

685 van Everdingen, R. O., Krouse, R. O., 1985. Isotope composition of sulphates generated by bacterial and abiological oxidation. Nature 315,

686   395–396.

687 Vaughan, D. G., Comiso, J. C., Allison, I., Carrasco, J., Kaser, G., Kwok, R., Mote, P., Murray, T., Paul, F., Ren, J., Rignot, E., Solomina, O.,

688   Steffen, K., Zhang, T., 2013. Observations: Cryosphere. In: Stocker, T. F., Qin, D., Plattner, M., Tignor, M., Allen, S. K., Boschung, J., Nauels,

689   A., Xia, Y., Bex, V., Midgley, P. M. (Eds.), Climate change 2013: The physical science basis. Contribution of Working Group I to the fifth

690   assessment report of the Intergovernmental Planel on Climate Change. Cambridge University Press, Cambridge, United Kingdom and New

691   York, NY, USA.

692 Wadham, J. L., Bottrell, S. H., Tranter, M., Raiswell, R., 2004. Stable isotope evidence for microbial sulphate reduction at the bed of a polythermal

693   high Arctic glacier. Earth Planet. Sci. Lett. 219, 341–355.

694 Wadham, J. L., Cooper, R. J., Tranter, M., Bottrell, S., 2007. Evidence for widespread anoxia in the proglacial zone of an arctic glacier. Chem.

695   Geol. 243, 1–15.

696 Wadham, J. L., Tranter, M., Skidmore, M., Hodson, A. J., Priscu, J., Lyons, W. B., Sharp, M., Wynn, P., Jackson, M., 2010. Biogeochemical

697   weathering under ice: size matters. Global Biogeochem. Cycles 24, GB3025.

698 Wagner, M., Roger, A. J., Flax, J. L., Brusseau, G. A., Stahl, D. A., 1998. Phylogeny of dissimilatory sulfite reductases supports an early origin of

699   sulfate respiration. J. Bacteriology 180, 2975–2982.

700 Wang, Q., Garrity, G. M., Tiedje, J. M., Cole, J. R., 2007. Naïve Bayesian classifier for rapid assignment of rRNA sequences into the new bacterial

701   taxonomy. Appl. Environ. Microbiol. 73, 5261–5267.

702 Wankel, S. D., Bradley, A. S., Eldridge, D. L., Johnston, D. T., 2014. Determination and application of the equilibrium oxygen isotope effect

703   between water and sulfite. Geochim. Cosmochim. Acta 125, 694–711.

704 Wolff-Boenisch, D., Gabet, E. J., Burbank, D. W., Langner, H., Putkonen, J., 2009. Spatial variations in chemical weathering and CO_2 consumption

705   in Nepalese High Himalayan catchments during the monsoon season. Geochim. Cosmochim. Acta 73, 3148–3170.

706 Wynn, P. M., Hodson, A., Heaton, T., 2006. Chemical and isotopic switching within the subglacial environment of a High Arctic glacier. Biogeo-

707   chemistry 78, 173–193.

708 Yde, J. C., Knudsen, N. T., 2004. The importance of oxygen isotope provenance in relation to solute content of bulk meltwaters at Imersuaq Glacier,

709   West Greenland. Hydrol. Process. 18, 125–139.

710   Yde, J. C., Riger-Kusk, M., Christiansen, H., Knudsen, N. T., Humlum, O., 2008. Hydrochemical characteristics of bulk meltwater from an entire

711   ablation season, Longyearbreen, Svalbard. J. Glaciol. 54, 259–272.

712   Ziaja, W., 2001. Glacial recession in Sørkappland and central Nordenskiöldbreen, Spitsbergen, Svalbard, during the 20th century. Arct. Antarct.

713   Alp. Res. 33, 36–41.

714   Ziaja, W., Pipała, 2007. Glacial recession 2001-2006 and its landscape effects in the Lindströmfjellet-Håbergnuten mountain ridge, Nordenskiöld

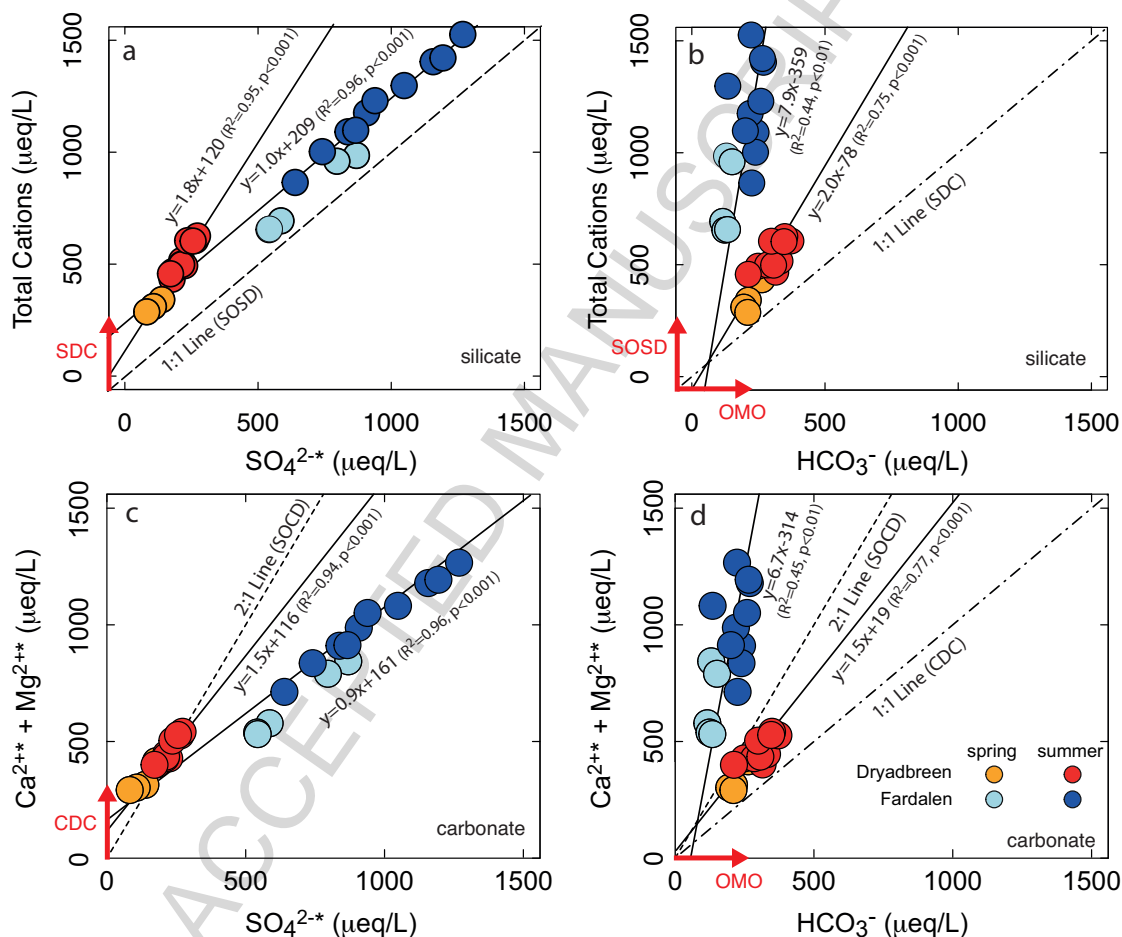715   Land, Spitsbergen. Pol. Polar Res. 28, 237–247.

Figure 6: Plots of total cations (Ca+Mg+Na+K) versus SO_4^{2-} (a) and HCO_3^- (b) together with $Ca^{2+}+Mg^{2+}$ versus SO_4^{2-} (c) and HCO_3^- (d). Concentrations have been corrected for precipitation inputs apart from HCO_3^- for which the correction is negligible. Orthogonal distance regression lines (solid) for each catchment (summer and spring points combined) together with the theoretical slopes (dashed and red arrows) describing idealised reactions are shown. Figures (a) and (b) depict idealised silicate weathering reactions assuming all the cations are from silicates. The 1:1 line in (a) (long dash) arises from sulfide oxidation coupled to silicate dissolution (SOSD, Eqn. 6). The 1:1 line in (b) (dot-dash) arises from carbonation of silicate (SDC, Eqn. 5). The vertical arrows in (a) and (b) indicate SDC (Eqn. 5) and SOSD (Eqn. 6) respectively i.e. cations are produced without SO_4^{2-}(SDC, Eqn. 5) or HCO_3^- (SOSD, Eqn. 6). Figures (c) and (d) depict idealised carbonate weathering reactions assuming Ca and Mg derive from carbonate only. The 2:1 line (short dash) in both figures represents the expected slope if the only weathering reaction occurring was sulfide oxidation coupled to carbonate dissolution (SOCD, Eqn. 4). This reaction can occur aerobically (Eqn. 4a) and anaerobically (Eqn. 4b). It is not possible to distinguish between the aerobic (Eqn. 4a) or anaerobic (Eqn. 4b) reaction based on reaction stoichiometry alone (Table 6). Note that depending of the exact formula of the reactant and product Fe species (e.g. Fe^{3+} vs $Fe(OH)_3$), slopes in $Ca^{2+}+Mg^{2+}$ vs SO_4 space greater than 2 are possible for the anaerobic reaction without changing the slope in $Ca^{2+}+Mg^{2+}$ vs HCO_3^- space (Tranter et al., 2002). The 1:1 line in (c) (dot-dash) arises from carbonation of carbonate (CDC, Eqn. 3). The vertical arrow in (c) indicates CDC (Eqn. 3) i.e. Ca^{2+} and Mg^{2+} are produced without HCO_3^-. The horizontal arrows in (b) and (d) indicate the production of HCO_3^- without cation release from organic matter oxidation (Eqn. 7). Theoretical and observed slopes are summarised in Table 6. Error bars are smaller than the symbols.
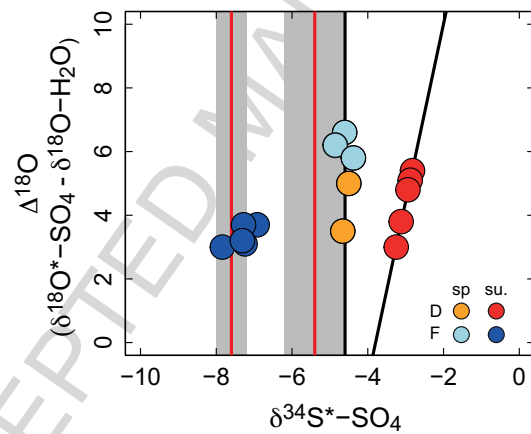
Figure 7: Plot of $\Delta^{18}O_{SO4-H2O}$ versus $\delta^{34}S^*$. In order to remove the effect of temporal variations in $\delta^{18}O_{H2O}$, $\Delta^{18}O_{SO4-H2O}$ is used. In the key sp. is spring su. is summer, D is Dryadbreen and F is Fardalen. The vertical red lines indicate the $\delta^{34}S$ values of measured pyrite mineral separates (Table 5) and the grey shading indicates the analytical error (2 SD) on those measurements. The vertical black line is an inferred $\delta^{34}S$ value of SO_4 derived from pyrite oxidation (Fig. 3). The correlation (R^2=0.99, p<0.001) between $\Delta^{18}O_{SO4-H2O}$ and $\delta^{34}S$ for Dryadbreen in summer (red points) suggests sulphate reduction and therefore an anoxic environment, however the magnitude of S isotope fractionation is not as great as would be expected for sulfate reduction (Seal II, 2006). Error bars are smaller than the symbols.

Highlights

Comparison of weathering processes in a glaciated and an unglaciated catchment
Combination of major elements, $\delta^{34}S$, $\delta^{18}O\text{-}SO_4$, $\delta^{18}O\text{-}H_2O$ and 16S-RNA
Mechanism of pyrite oxidation differed between the two catchments
No evidence for sulfate reduction